Title

A MEASUREMENT OF THE K (89O) MASS DIFFERENCE IN THE REACTIONS n+d ->(p)AK*+ AND n-p ->K*|

Author

Hoch, Paul L.

Publication Date

1972-10-01

LBL-1053
c.1

A MEASUREMENT OF THE $K^*(890)$ MASS DIFFERENCE IN THE REACTIONS $\pi^+ d \to (p)\Lambda K^{*+}$ AND $\pi^- p \to \Lambda K^{*0}$

Paul L. Hoch
(Ph. D. Thesis - Part 3)

October 16, 1972

Prepared for the U.S. Atomic Energy Commission under Contract W-7405-ENG-48

LBL-1053
c.1

DISCLAIMER

A MEASUREMENT OF THE K*(890) MASS DIFFERENCE IN THE REACTIONS $\pi^+ d \to (p)\Lambda K^{*+}$ AND $\pi^- p \to \Lambda K^{*o}$

[This report is Chapter 4 of a Ph. D. thesis,]
[the other parts of which are LBL Reports LBL-1051 and LBL-1052.]

CONTENTS

A MEASUREMENT OF THE $K^*(890)$ MASS DIFFERENCE IN THE REACTIONS $\pi^+ d \to (p)\Lambda K^{*+}$ AND $\pi^- p \to \Lambda K^{*o}$

Paul L. Hoch

Lawrence Berkeley Laboratory
University of California

ABSTRACT

We have attempted to measure the $K^*(890)$ electromagnetic mass difference in two charge-symmetric pairs of $\pi N \to \Lambda K^*$ reactions. Using data from bubble chamber exposures at $E_{c.m.} = 2$ to 3 GeV, we have done maximum-likelihood fits to the $\Lambda K\pi$ final states, approximating the peak in $m(K\pi)$ by a simple fixed-width Breit-Wigner. We report a mass difference of $\Delta m \equiv m(K^{*o}) - m(K^{*\pm}) = (-2.7 \pm 4.4)$ MeV; this error is twice the statistical error from the fitting program.

The present world average, with this result included, is $\Delta m = (5.2 \pm 1.4)$ MeV. We feel that our result is comparable in quality to those which had been reported when we began this study. The use of charge-symmetric reactions was intended to reduce one possible source of systematic error: peak shifts due to interference with background should cancel in the mass difference. Various systematic effects and statistical limitations have prevented us from getting a good result by this simple expedient, and have apparently given the wrong answer. Our result is inconsistent both with those early results and with a recent and precise determination using a high-statistics, interference-free sample.

4.1 INTRODUCTION

In the 1970 Particle Data Group (PDG) review of particle properties, the relatively poor status of the measurement of the K*(890) mass difference was noted.[181] In particular, it was pointed out that no result had been published exploiting charge symmetry to eliminate peak shifts due to interference. At Art Rosenfeld's suggestion, we have examined the data from our $\pi^+ d$ exposure (Pi66) and (for charge-symmetric final states) from an earlier LBL $\pi^- p$ exposure (Pi63). Our results are summarized in the next section, with details left for Section 4.3. In Section 4.4 we evaluate our result and compare it with other determinations.

4.11 SIGNIFICANCE OF Δm

CPT invariance requires $m(K^{*o}) = m(\bar{K}^{*o})$, and $m(K^{*+}) = m(\bar{K}^{*-})$. The mass difference between the members of each kaon doublet is an electromagnetic effect; it is of interest because it can be related by simple SU(3) to other electromagnetic mass-splitting effects in the vector-meson nonet.

These relations have been set forth in detail by S. Flatté;[182] only the results are noted here. Making only the usual assumption that the electromagnetic current transforms like a U-spin scalar, one finds that

$$-\sqrt{3}\,\sin\theta\, M_{\rho\omega} + \sqrt{3}\,\cos\theta\, M_{\rho\phi} = [m(K^{*+})-m(K^{*o})] - [m(\rho^+)-m(\rho^o)]$$

where θ is the ω-ϕ mixing angle and $M_{\rho\omega} \equiv \langle\rho|M|\omega\rangle$ is the matrix element of the electromagnetic mass-splitting operator.

In the quark model, $\sin\theta = +1/\sqrt{3}$ and $M_{\rho\phi} = 0$, so this equation reduces to

$$M_{\rho\omega} = [m(K^{*o})-m(K^{*+})] - [m(\rho^o)-m(\rho^+)]$$

From ρ-ω interference, Biggs *et al.* have found $|M_{\rho\omega}| = (1.9 \pm 0.4)$ MeV.[183] There are well-known difficulties in measuring the mass and width of the ρ; the PDG compilation lists just one measurement of the mass difference, $m(\rho^o)-m(\rho^\pm) = (2.4 \pm 2.1)$ MeV.[184] This leads to the prediction $\Delta m \equiv m(K^{*o})-m(K^{*\pm}) = [(4.3 \text{ or } 0.5) \pm 2.1]$ MeV.

We note that additional theoretical assumptions lead to both positive and negative values for Δm. For example,[185]

(1) The assumption that isospin-2 effects are small implies small ρ mass splittings; with additional assumptions, a value for $M_{\rho\omega}$ can be calculated, leading to $m(K^{*o})-m(K^{*\pm}) \approx M_{\rho\omega} \approx -2.5$ MeV.[186]

(2) Both Duimio and Scotti[187] and Bose[188] predict $m(K^{*o})-m(K^{*\pm}) < 0$.

(3) A quark model-SU(6) treatment gives $m(K^{*o})-m(K^{*\pm}) = m(K^o)-m(K^\pm)$ [=(+3.95 ± 0.13) MeV].[189,190]

4.12 PREVIOUS EXPERIMENTAL STATUS

As we shall see in detail in Section 4.33, the peak of a Breit-Wigner can easily be shifted by a substantial fraction of Γ due to interference between the resonant amplitude and a nonresonant background. Since the mass splitting under consideration seems to be a small fraction of the width, which is about 50 MeV, this effect must be taken into account unless the background is very small. Any single determination of the K^* masses is also subject to other possible systematic errors, such as the effects of looking at different final-state topologies.

For these reasons, one cannot expect to get a meaningful value for the mass difference by simply subtracting the "established" values for the individual masses. In fact, the tabulated values for the mass of the K^{*o} are inconsistent with each other, which in itself indicates systematic errors. After scaling the errors in these determinations by a factor of 1.3, the PDG reported[191]

$$m(K^{*o}) = (893.93 \pm 0.73)\ \text{MeV}; \quad m(K^{*\pm}) = (892.05 \pm 0.38)\ \text{MeV}.$$

Without detailed examination of the various experiments which contribute to these mass values, the best one can do is hope that interference and other systematic effects tend to cancel and that there might be some significance to the difference, which was $\Delta m = (+1.88 \pm 0.83)$ MeV. (The most recent compiled mass values give $\Delta m = (4.74 \pm 0.84)$ MeV.[184])

When this work was begun, the PDG listed only three papers which reported a value for the mass difference. The PDG pointed out that some of these had unreasonably small errors and that they were subject to interference effects. By using charge-symmetric reaction pairs, we have reduced that problem. After this work was completed, Aguilar-Benitez *et al.* reported what seems to be a definitive study of the mass difference, based on a high-statistics, low-background K^* sample. In Section 4.4 we will consider these results in some detail, and comment on possible systematic errors compared to those in our determination.

4.2 RESULTS OF THIS ANALYSIS

We have examined data from 1.9 to 3.0 GeV for two charge-symmetric pairs of $\pi N \rightarrow \Lambda K \pi$ reactions. Our intention was to do what was expected to be a quick and easy study, using data that was already available, and exploiting the charge symmetry as much as possible.

The $K^*(890)$ is an I=1/2 P-wave resonance; if it is accompanied by an I=3/2 amplitude, the peak in the $m(K\pi)$ spectrum can be shifted from the K^* mass. (A non-P-wave amplitude with I=1/2 can give interference effects in the K^* decay distribution, but not in the mass spectrum.) The charge symmetry of strong interactions requires that the amplitude be the same for the π^-p reaction and the I_z-reflected π^+n reaction. Therefore, at any particular c.m. energy, the peak shift due to interference with background cancels out in the mass difference.

On the other hand, we have the disadvantage of having to combine two different experiments (albeit in the same bubble chamber) and, in order to get adequate statistics, having to compare the charge-symmetric reactions over a rather wide c.m. energy band. Once it became apparent that the determination of the K^* masses to within a few MeV from our data might not be feasible at all, we decided not to pursue various systematic biases.

The motivation behind the choice of reactions studied and the cuts made is presented in Section 4.31. We fit the Dalitz plot variables to phase space plus simple Breit-Wigners for the K^* and $Y^*(1385)$, varying the relative amounts of each process and the resonance masses.

Here we present the three independent measurements of Δm which we have decided to use in our final value:

Reactions		$E_{c.m.}$	$m(K^{*+})$	$m(K^{*0})$	Δm
$\pi^+n \rightarrow$	$\pi^-p \rightarrow$	(GeV)	(MeV)	(MeV)	(MeV)
$\Lambda K^+\pi^0$	$\Lambda K^0\pi^0$	$\approx$1.9 to 2.4	902.3 ± 8.0	895.3 ± 4.5	−7.0 ± 9.1
$\Lambda K^0\pi^+$	$\Lambda K^+\pi^-$	$\approx$1.9 to 2.4	884.4 ± 3.0	889.1 ± 1.7	+4.7 ± 3.5
$\Lambda K^0\pi^+$	$\Lambda K^+\pi-$	2.4 to $\approx$3.0	901.5 ± 2.7	893.4 ± 1.6	−8.1 ± 3.1

The average of these three results is $\Delta m = (-2.7 \pm 2.2)$ MeV, with a χ^2 of 7.7 for 2 degrees of freedom. For reasons given in Section 4.35, we decided even before the average was calculated that the quoted errors were too small by about a factor of 2. Thus, we introduce a "scale factor" of 2 and report

$$\Delta m = (-2.7 \pm 4.4) \text{ MeV}.$$

The following points are discussed at greater length below:

(1) We have not used events with an invisible spectator proton as well as a π^0 or an undetected K^0. This "pseudo-one-constraint" cut improves the general charge-symmetric appearance of the reaction pairs.

(2) Since we did not have identical c.m. energy distributions for the reaction pairs, we divided the sample into regions of "low" and "high" energy.

(3) We did not use the result for the high-energy interval of the first reaction pair listed above. (The fit was not good. If it is included, the average, without scaling the error, is (-0.8 ± 2.2) MeV.)

(4) The errors in the table are those calculated by the maximum-likelihood fitting program. Nothing has been added for systematic effects. The obvious limitation should be emphasized: this error simply reflects the behavior of the likelihood function when the K^* mass is changed. It does not indicate the quality of the fit or the validity of the model. The fits are no better than adequate in the K^* region.

The data and the results of the fits are presented in Tables 4.1 through 4.4 and Figures 4.1 through 4.7. The events are tallied in Table 4.1. Tables 4.2 and 4.3 give the results of the fits for the resonance masses and their differences. Table 4.4 presents similar results for the resonance amounts. Figures 4.1 through 4.4 show the two-body mass spectra and the c.m. energy distribution for the fits covering all energies. (The dotted curves were generated by a Monte-Carlo method to illustrate the fits; the fitting procedure did not use the Monte-Carlo events.) Figure 4.5 shows the $m(K\pi)$ spectra with the pseudo-one-constraint cut; compare Fig. 4.1. Figures 4.6 and 4.7 correspond to the low-and high-energy parts of Figure 4.1.

	$\pi^+n \rightarrow \Lambda K^+\pi^0$	$\pi^-p \rightarrow \Lambda K^0\pi^0$	$\pi^+n \rightarrow \Lambda K^0\pi^+$	$\pi^-p \rightarrow \Lambda K^+\pi^-$
Total number of Events	2058	1206	2485	3085
By Visible Decays: Λ,K	140 (1C)	1206 (1C)	528 (4C)	187
Λ only	1918 (1C)	-	1448 (1C)	2711
K only	-	-	509 (1C)	187
With p_{sp} - Fid Cut:	1434	994	1458	2600
By $E_{c.m}$ - E < 2.4 GeV	695	584	652	1193
E > 2.4 GeV	739	410	806	1407
With "Pseudo-1C Cut" also:	479	994	878	2600
By $E_{c.m.}$ - E < 2.4 GeV	225	584	400	1193
E > 2.4 GeV	254	410	478	1407

Event Tally

Table 4.1

Reaction	1C Cut?	m(K*) (MeV) E<2.4 GeV	E>2.4 GeV	Average of Low, High E	χ^2 2 d.f.	All E (Fit)
$\pi^+n\rightarrow\Lambda K^+\pi^o$	No	903.0 ± 4.9	869.0 ± 4.4	884.2 ± 3.3	(26.6)	895.0 ± 3.3
"	Yes	902.3 ± 8.0	874.7 ± 6.7	886.1 ± 5.1	(7.0)	894.8 ± 4.9
$\pi^-p\rightarrow\Lambda K^o\pi^o$	-	895.3 ± 4.5	900.8 ± 5.0	897.8 ± 3.3	(0.7)	897.1 ± 3.3
$\pi^+n\rightarrow\Lambda K^o\pi^+$	No	890.3 ± 2.6	895.9 ± 2.1	893.7 ± 1.7	(2.7)	893.7 ± 1.7
"	Yes	884.4 ± 3.0	901.5 ± 2.7	894.0 ± 2.0	(18.0)	894.2 ± 2.0
$\pi^-p\rightarrow\Lambda K^+\pi^-$	-	889.1 ± 1.7	893.4 ± 1.6	891.5 ± 1.1	(3.5)	891.7 ± 1.1

Reaction	1C Cut?	m(Y*) (MeV) E<2.4 GeV	E>2.4 GeV	Average of Low, High E	χ^2 2 d.f.	All E (Fit)
$\pi^+n\rightarrow\Lambda K^+\pi^o$	No	1385. ± 2.1	1382. ± 3.6	1384. ± 1.8	(0.5)	1384. ± 1.8
"	Yes	1382. ± 3.8	1375. ± 5.1	1380. ± 3.0	(1.2)	1380. ± 3.0
$\pi^-p\rightarrow\Lambda K^o\pi^o$	-	1378. ± 2.2	1379. ± 3.2	1378. ± 1.8	(0.1)	1378. ± 1.8
$\pi^+n\rightarrow\Lambda K^o\pi^+$	No	1379. ± 2.4	1382. ± 7.9	1379. ± 2.3	(0.1)	1380. ± 2.5
"	Yes	1380. ± 3.0	1377. ± 8.8	1380. ± 2.9	(0.1)	1379. ± 3.1
$\pi^-p\rightarrow\Lambda K^+\pi^-$	-	1388. ± 1.8	1378. ± 5.3	1387. ± 1.7	(3.2)	1386. ± 1.9

K* and Y* Masses

Table 4.2

$\Delta m(K^*) \equiv m(K^{*o}) - m(K^{*+})$ (MeV)

Reactions $\pi^+n\to/\pi^-p\to$	1-C Cut?	Low E <2.4 GeV	High E >2.4 GeV	Weighted Average	(χ^2) (2 d.f.)	All E (From fit)
$\Lambda K^+\pi^o/\Lambda K^o\pi^o$	No	-7.7 ± 6.7	31.8 ± 6.7	12.0 ± 4.7	(17.6)	2.1 ± 4.6
"	Yes	-7.0 ± 9.1	26.1 ± 8.4	11.0 ± 6.2	(7.1)	2.3 ± 5.9
$\Lambda K^o\pi^+/\Lambda K^+\pi^-$	No	-1.2 ± 3.1	-2.5 ± 2.6	-2.0 ± 2.0	(0.1)	-2.0 ± 2.0
"	Yes	$+4.7 \pm 3.5$	-8.1 ± 3.1	-2.5 ± 2.3	(7.6)	-2.5 ± 2.3

$\Delta m(Y^*) \equiv m(Y^* \text{ in } \pi^-p) - m(Y^* \text{ in } \pi^+n)$ (MeV)

(A) $\Delta m(Y^*) = m(Y^{*o} \text{ in } \pi^-p) - m(Y^{*o} \text{ in } \pi^+n)$; should be 0:

$\Lambda K^+\pi^o/\Lambda K^o\pi^o$	No	$-7. \pm 3.0$	$-3. \pm 4.8$	$-6. \pm 2.5$	(0.5)	$-6. \pm 2.5$
"	Yes	$-4. \pm 4.4$	$+4. \pm 6.0$	$-1. \pm 3.5$	(1.2)	$-2. \pm 3.4$

(B) $\Delta m(Y^*) = m(Y^{*-}) - m(Y^{*+})$:

$\Lambda K^o\pi^+/\Lambda K^+\pi^-$	No	$+9. \pm 3.0$	$-4. \pm 9.5$	$+8. \pm 2.8$	(1.7)	$+6. \pm 3.1$
"	Yes	$+8. \pm 3.5$	$+1. \pm 10.$	$+7. \pm 3.3$	(0.4)	$+7. \pm 3.6$

K^* and Y^* Mass Differences

Table 4.3

		K^* Fraction (%)			Y^* Fraction (%)		
Reaction	1-C Cut?	Low E <2.4 GeV	High E >2.4 GeV	All E	Low E <2.4 GeV	High E >2.4 GeV	All E
$\pi^+n\rightarrow\Lambda K^+\pi^o$	No	20.5 ± 3.3	16.2 ± 2.2	15.3 ± 1.8	34.4 ± 3.3	13.6 ± 1.8	18.0 ± 1.6
"	Yes	23.1 ± 5.6	18.4 ± 3.7	19.0 ± 3.1	33.4 ± 5.4	18.9 ± 3.3	20.7 ± 2.7
$\pi^-p\rightarrow\Lambda K^o\pi^o$	-	22.1 ± 3.5	19.1 ± 3.0	19.6 ± 2.2	38.8 ± 3.3	24.9 ± 3.0	28.0 ± 2.2
$\pi^+n\rightarrow\Lambda K^o\pi^+$	No	44.8 ± 3.7	41.2 ± 2.4	40.0 ± 2.0	25.8 ± 2.9	4.7 ± 1.2	10.8 ± 1.3
"	Yes	50.7 ± 4.7	44.4 ± 3.2	44.9 ± 2.7	25.7 ± 3.8	5.0 ± 1.6	10.8 ± 1.6
$\pi^-p\rightarrow\Lambda K^+\pi^-$	-	49.1 ± 2.5	44.1 ± 1.8	43.9 ± 1.5	29.4 ± 2.2	5.3 ± 1.0	13.1 ± 1.1

		ΔK^* Fraction (%)			ΔY^* Fraction (%)		
Reactions	1-C	Low E	High E	All E	Low E	High E	All E
$\pi^+n\rightarrow/\pi^-p\rightarrow$	Cut?	<2.4 GeV	>2.4 GeV		<2.4 GeV	>2.4 GeV	
$\Lambda K^+\pi^o/\Lambda K^o\pi^o$	No	1.6 ± 4.8	2.8 ± 3.7	4.3 ± 2.8	4.4 ± 4.7	11.3 ± 3.5	10.0 ± 2.7
"	Yes	-1.0 ± 6.6	0.7 ± 4.8	0.5 ± 3.8	5.4 ± 6.4	6.0 ± 4.5	7.3 ± 3.4
$\Lambda K^o\pi^+/\Lambda K^+\pi^-$	No	4.3 ± 4.5	3.0 ± 3.1	3.9 ± 2.5	3.6 ± 3.6	0.6 ± 1.6	2.3 ± 1.7
"	Yes	-1.6 ± 5.3	-0.3 ± 3.7	-1.0 ± 3.1	3.8 ± 4.3	0.3 ± 1.9	2.4 ± 1.9

Resonance Fractions and Differences

Table 4.4

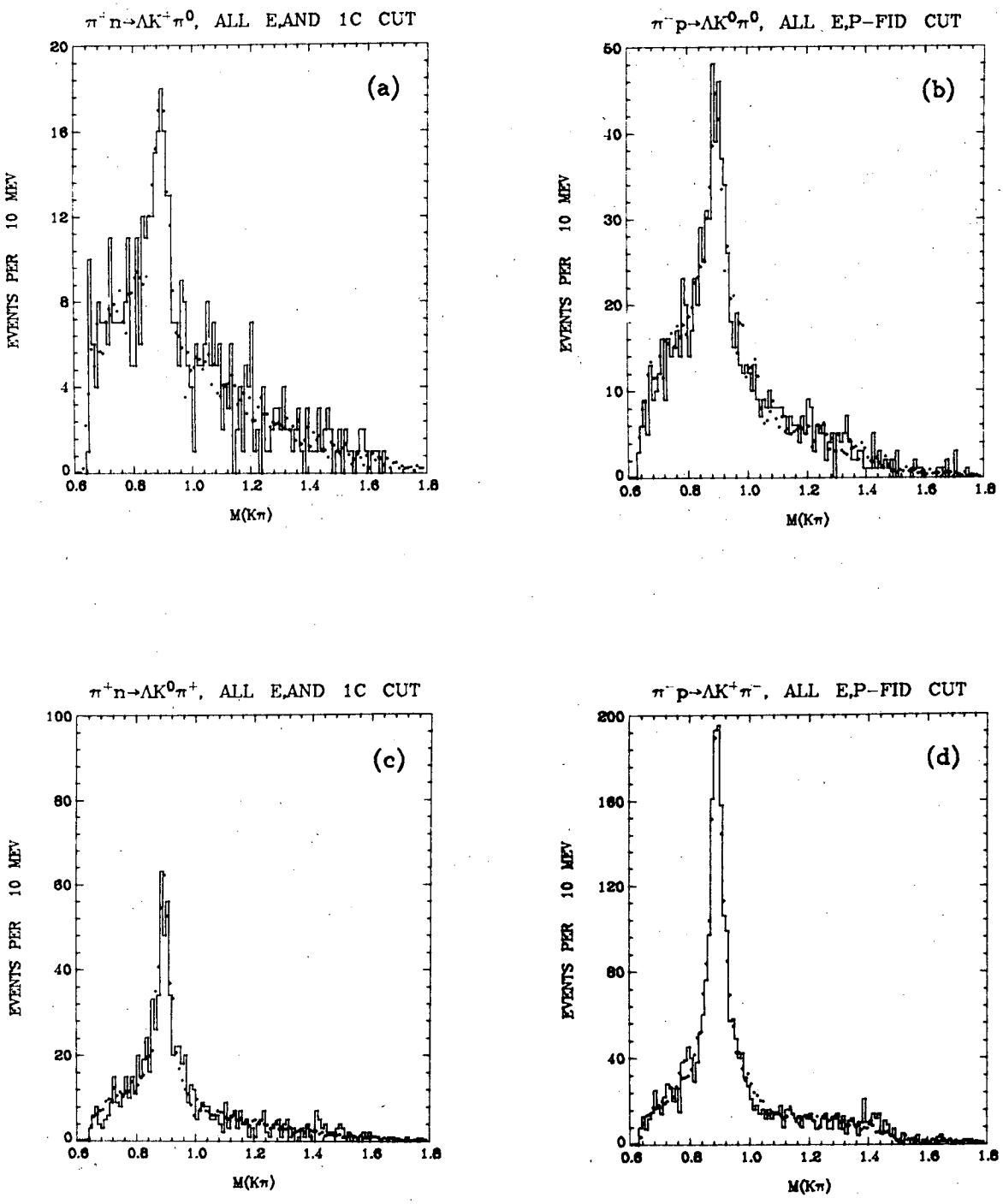

XBL 729-1794

Fig. 4.1

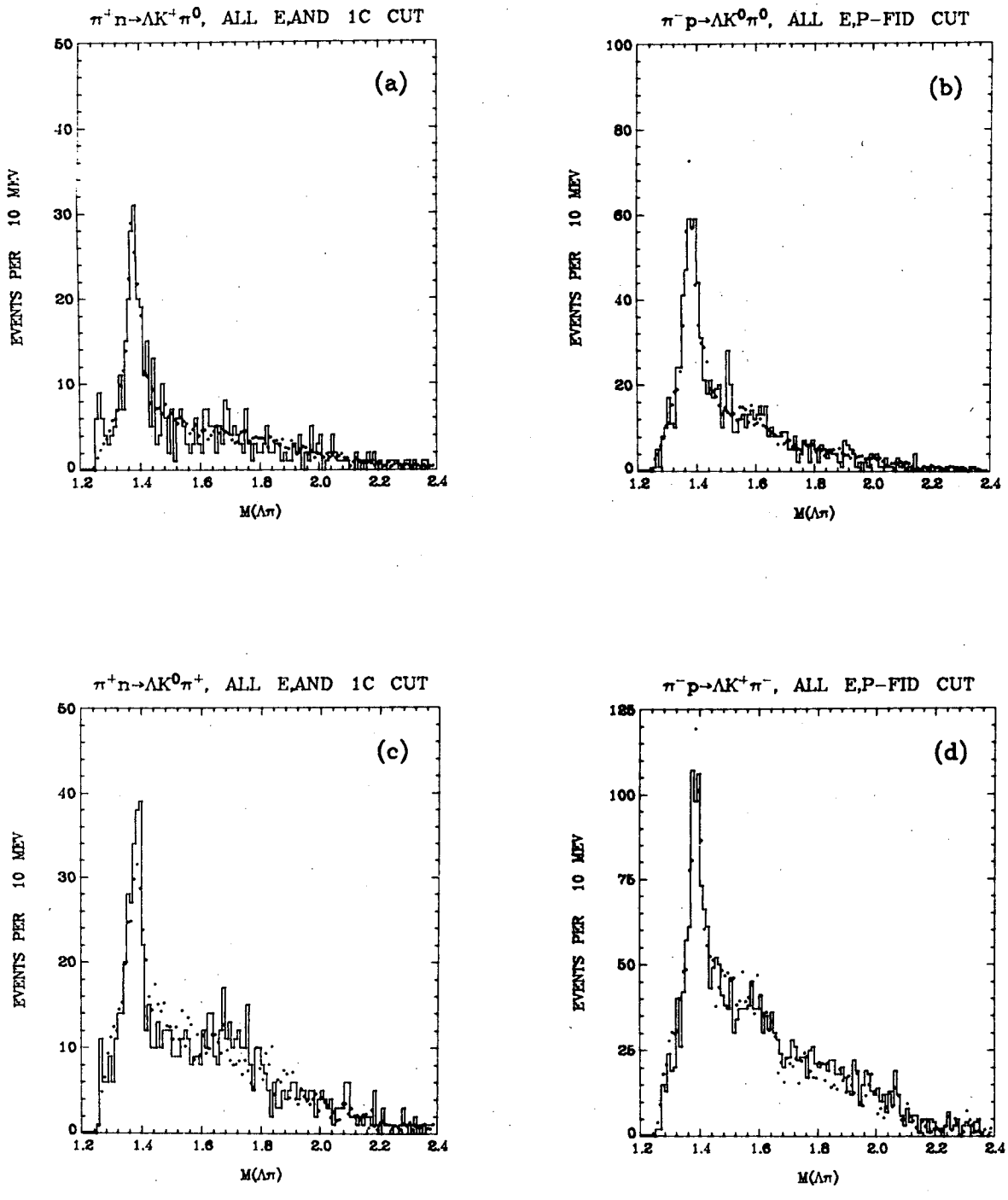

XBL 729-1795

Fig. 4.2

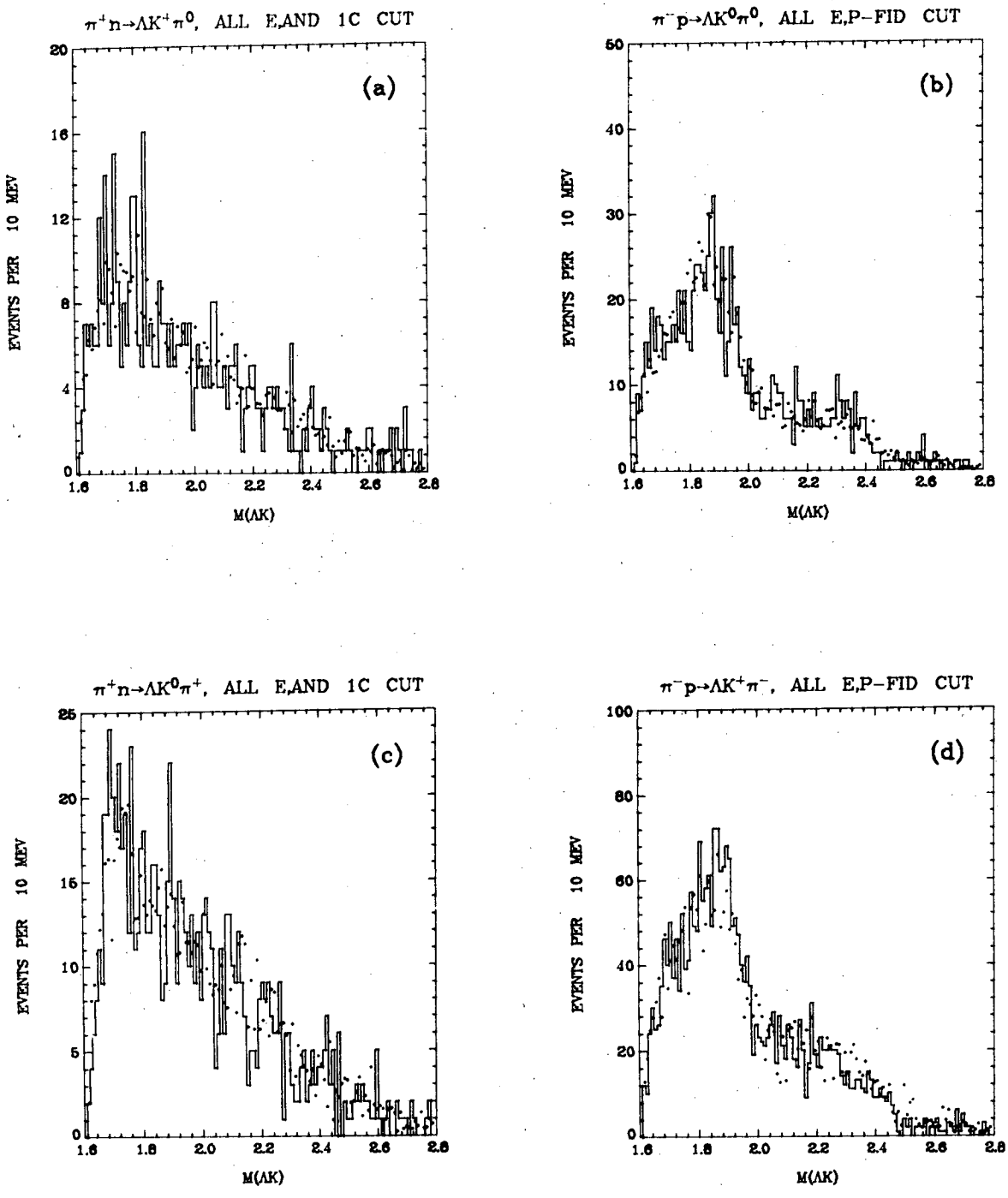

XBL 729-1796

Fig. 4.3

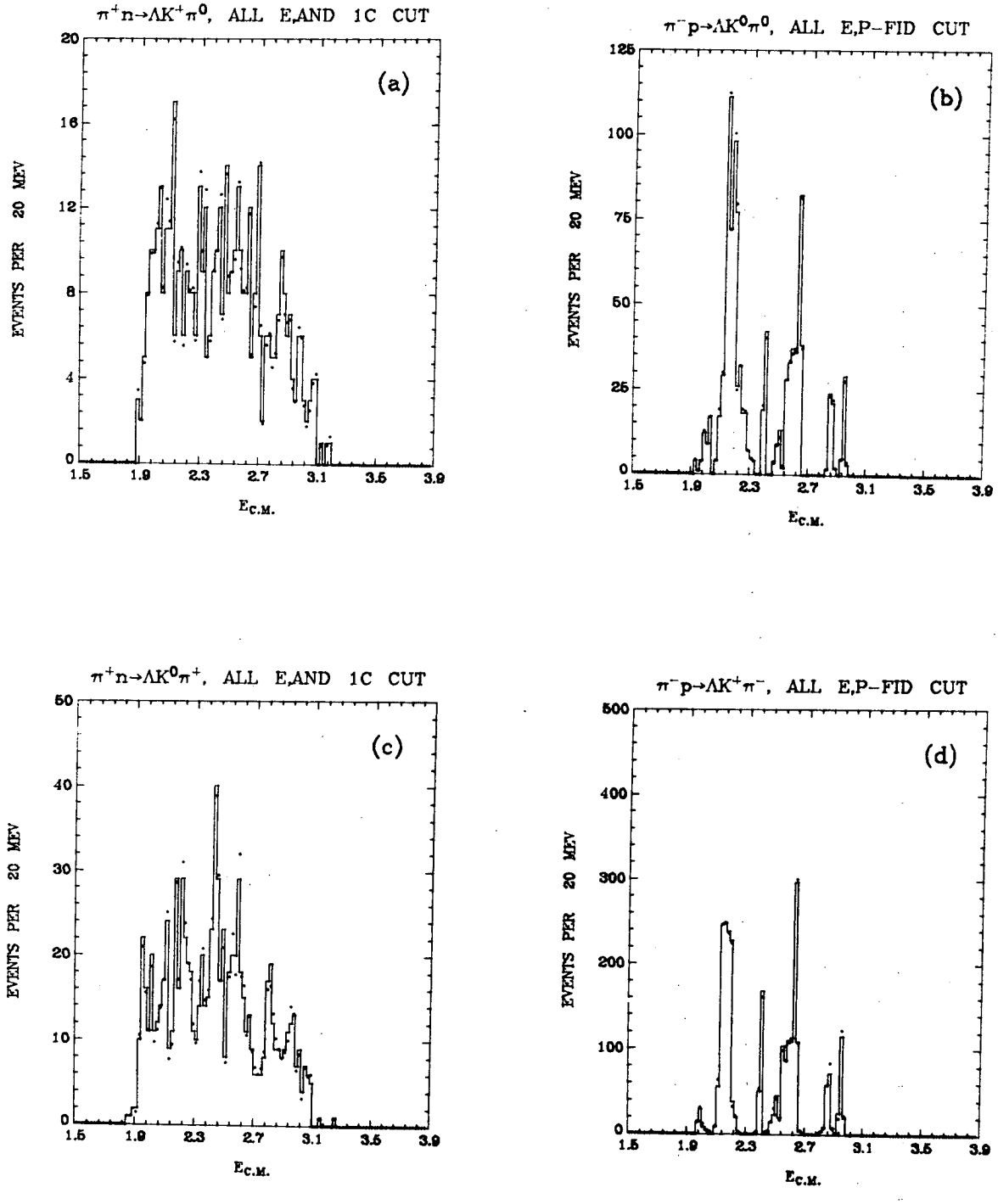

XBL 729-1797

Fig. 4.4

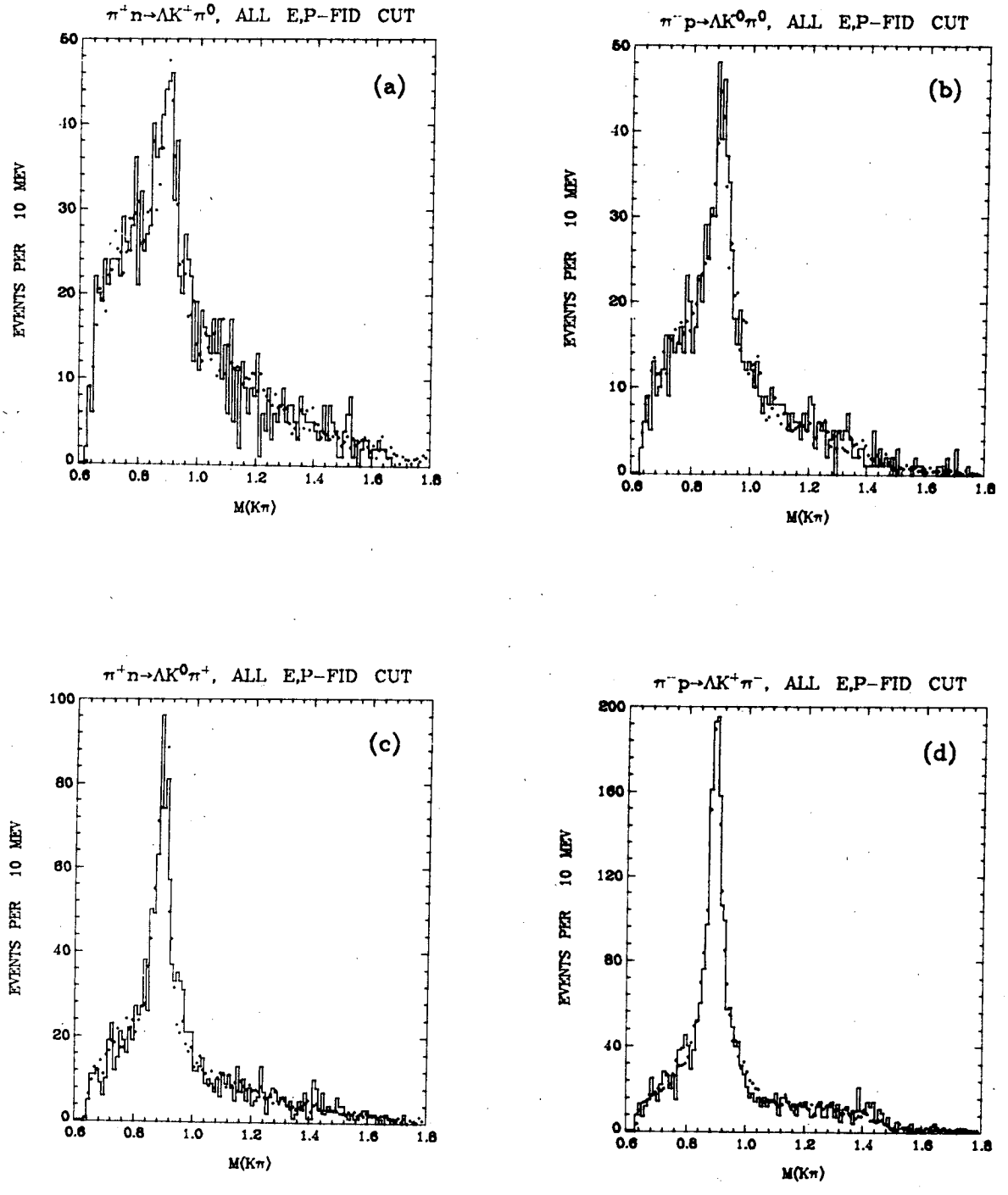

XBL 729-1798

Fig. 4.5

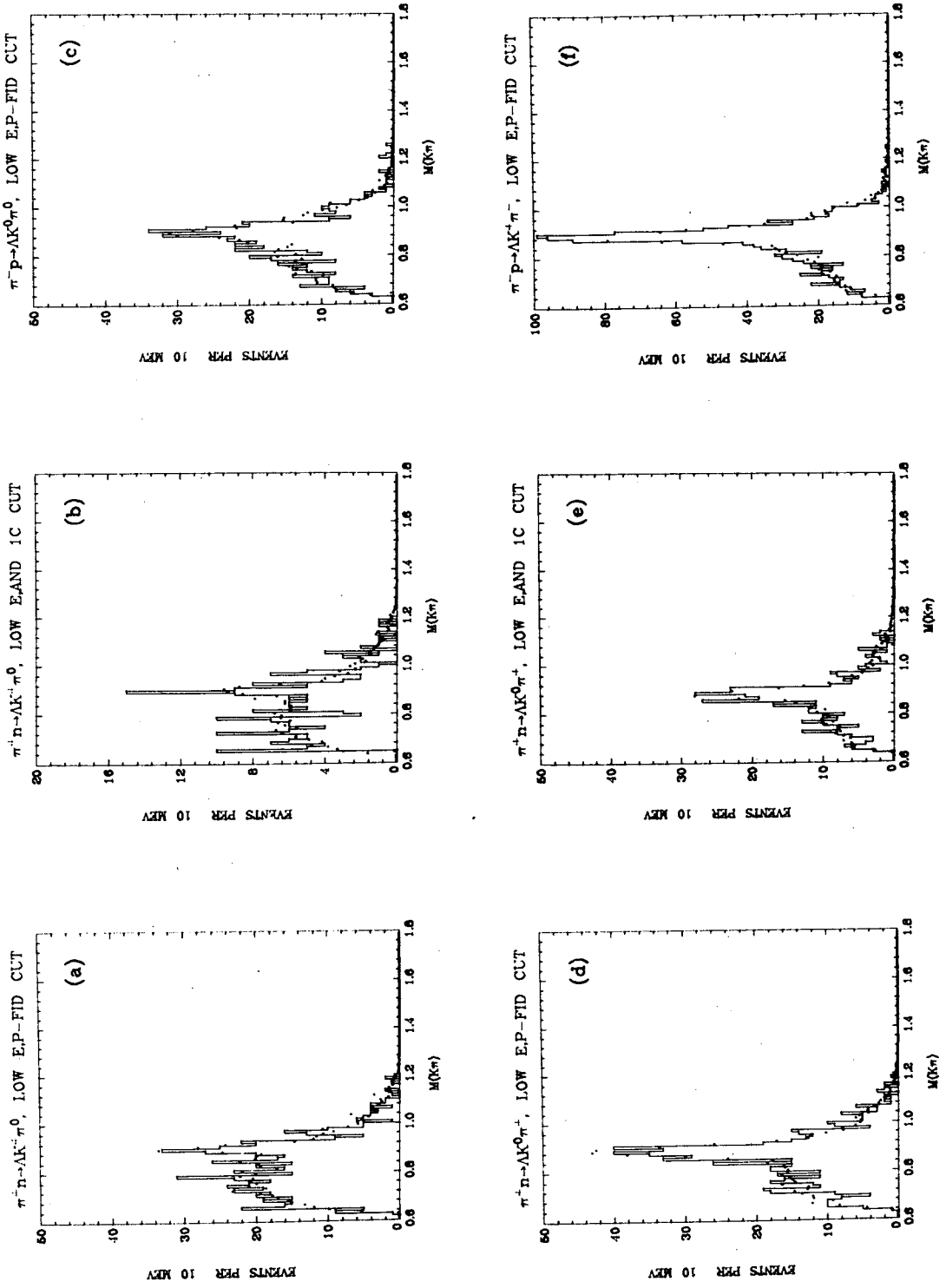

XBL 729-1799

Fig. 4.6

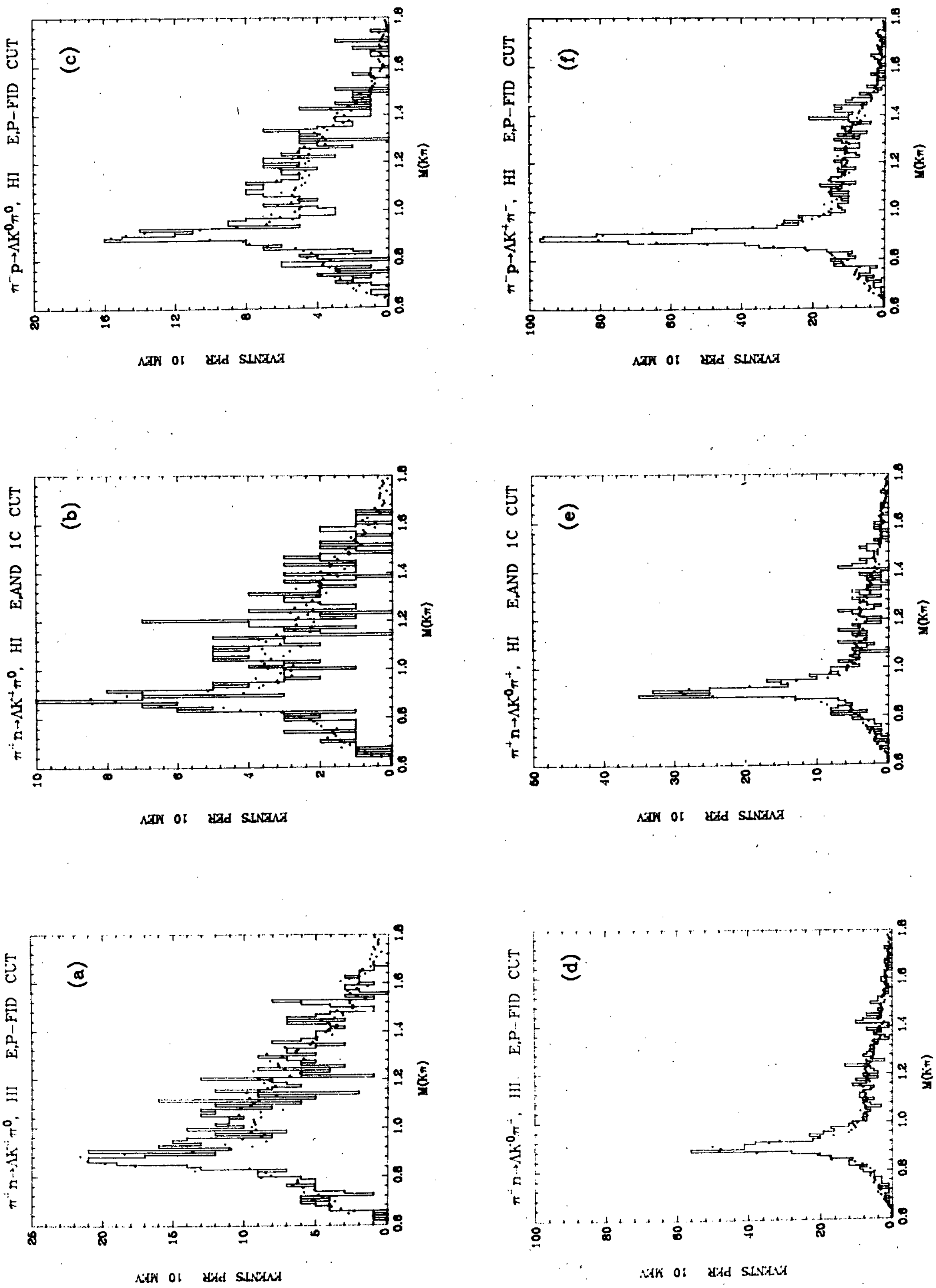

XBL 729-1800

Fig. 4.7

4.3 DETAILS

4.31 THE DATA SAMPLE AND THE CUTS IMPOSED

Table 4.1 gives the number of events in our data for all reactions of the form $\pi^- p$ or $\pi^+ n$ (with a spectator proton) $\rightarrow \Lambda K \pi$. Those reactions are

$$\pi^+ n \longrightarrow \Lambda K^+ \pi^0 \qquad (4.1)$$

$$\pi^- p \longrightarrow \Lambda K^0 \pi^0 \qquad (4.2)$$

$$\pi^+ n \longrightarrow \Lambda K^0 \pi^+ \qquad (4.3)$$

$$\pi^- p \longrightarrow \Lambda K^+ \pi^- \qquad (4.4)$$

Separate tallies are shown for the different visible decays, and the number of kinematic constraints at the production vertex is given.

The $\pi^+ n$ events come from a $\approx$20 ev/μb $\pi^+ d$ exposure (referred to as Pi66A) in the 72-inch bubble chamber at beam momenta from 2.7 to 4.2 GeV/c. They have been assigned to the competing final states according to the scheme which is described in Chapter 2.[192] Highly-constrained fits were favored via a bias in X^2; hypotheses with the same number of kinematic constraints were separated according to X^2. We have also used events from a companion $\pi^+ d$ exposure at 1.1 to 2.4 GeV/c (Pi66B), the processing of which is described in Don Davies' thesis.[193] The $\pi^- p$ sample comes from an older 72-inch bubble chamber exposure (Pi63). We used the events as they were originally processed.[194]

Table 4.1 also gives the number of events which survive the various cuts that have been applied in the fitting program. In the mass-spectra plots (Figs. 4.1 - 4.7), these cuts are denoted by "P-FID CUT", "AND 1C CUT", "LOW E", and "HI E". These cuts are described and motivated here.

"P-FID CUT" (Spectator proton and fiducial volume cuts)

As is customary, we discarded $\pi^+ d$ events where the spectator proton has a fitted lab momentum of greater than 300 MeV/c. This is expected to eliminate most events which can not be treated as $\pi^+ n$ with a true spectator proton (e.g., those which results from double scattering), and it should also reduce the contamination from other final states. Also, the usual fiducial-volume cut is made, requiring the production and decay vertices to be reasonably far from the chamber edges.[195] This "P-FID CUT" was applied to all of the fits presented in this report.

As noted in Section 2.7, the fiducial-volume cut is accompanied by an appropriate weight, calculated for each surviving event. We did not use weighted events in the fits (essentially for convenience). Although the average weight

can be quite different from 1 for some of the final states, the weight is not correlated with m(Kπ). This was confirmed by examination of weighted and unweighted mass spectra, and by calculation of the average weight for each 10 MeV bin in m(Kπ).

"LOW [HI] E" (C.m. energy cut)

The principle of charge symmetry relates amplitudes at the same total energy. As shown by the energy spectra in Figure 4.4, the π^+n and π^-p experiments cover roughly the same range, essentially 1.9 to 3.1 GeV. However, the energy spectra for charge-symmetric reactions are nowhere near identical. (Even if the incident beam momenta had been the same, the deuteron Fermi motion would have spread out the π^+n effective c.m. energy.) Because of the small number of events available, we restricted our consideration of energy-dependent effects to dividing the data into two energy intervals. The dividing line between "LOW E" and "HI E" was arbitrarily chosen to be 2.4 GeV (which corresponds to a beam momentum of 2.6 GeV/c).

We ran the fits on all events as well as on each energy interval separately. Table 4.2 presents the results for the masses of the K^* and Y^*, together with the weighted averages of the low- and high-energy results. We see that in all cases but the first two, the weighted average agrees very well with the fit using all events. (The exception is $\pi^+n \rightarrow \Lambda K^+\pi^0$ at high energy, where the K^* mass comes out unreasonably low; this result was not used, as noted earlier.) The additional information that we obtained by fitting the two energy regions separately is that the (apparent) K^* masses in general differ significantly in the two fits. On the other hand, the apparent Y^* mass shows little such variation. One possible interpretation of these results is that the K^* peak is shifted by interference with background, while Y^* production can not be similarly affected (since $\Lambda\pi$ is pure I=1). If this is the case, perhaps even smaller energy intervals must be used before a good result can be obtained; in any case it confirms that peak shifting cannot be ignored. However, without further work we cannot conclude that the mass variations are not due to systematic effects or inadequacies of the model used in the fit.

"1C CUT" (Removal of events with a pseudo-one-constraint fit)

It is well known that there are deficiencies in our treatment of odd-prong events - i.e., those where the spectator proton is too slow to leave a measurable track. (See Section 2.10.) We treat the invisible proton as if it had measured momentum components of zero, with appropriate errors. This degrades the fits (that is, it increases the possibility of misassignment, as if the number of constraints had been reduced, and introduces artificial correlations), but it is quite adequate for fits that have no other unmeasured particles. However, for fits that would be one-constraint (at the production vertex) if the spectator were visible, there is a strong correlation between the fitted momenta of the invisible spectator and of the unseen neutral. Since the spectator is roughly isotropic in the lab, this correlation can distort the invariant mass spectra involving the unseen neutral. Thus, we defined a "pseudo-1C cut", which deletes all events where there is an invisible spectator and a π^0 or a K^0 which is not seen to decay. (It was felt that the K^* mass would probably not be affected in 1-C fits where the unseen particle was not one of the decay products of the K^*.)

We have tabulated our results both without and with this cut. (Table 4.3; Fig. 4.5-4.7) Here we note two indicators that this cut should be made. First, the shapes of the overall mass spectra are changed so that the pairs of reactions look more similar. Included in Table 4.4 are the fractions of K^* and Y^* production from each fit. (Since the c.m. energy spectra are not identical, the coefficients of the resonance terms should not necessarily be the same in charge-symmetric pairs; the resonance fraction is the integral of the corresponding term of the matrix element over phase space.) Note that when the "1C CUT" is applied, the fractional resonance production agrees quite well for the charge-symmetric resonance pairs.

In addition, we observe that in reaction (4.1), this cut should clean up the Y^* as well as the K^*, since the π^0 is in both resonances. In fact, the difference between the Y^{*0} mass as measured in reactions (4.1) and (4.2) is brought significantly closer to zero. From reactions (4.3) and (4.4), we get values of $\Delta m(Y^*) \equiv m(Y^{*-}) - m(Y^{*+})$ which are consistent with the accepted value of $(+3 \pm 2)$ MeV.[196] The pseudo-1-C cut makes no significant difference in $\Delta m(Y^*)$; none was expected, since the 1-C cut involves only events in reaction (4.3) with an unseen K^0. It is reassuring to note the agreement of the Y^* mass differences with the expected results; however, such observations are no substitute for a thorough study of the systematic effects which may be present.

Although some of the values for $\Delta m(K^*)$ at low or high energy are changed by the 1-C cut, the values for all energies together are not significantly affected. As noted above, we choose to report only the results with the 1-C cut.

4.32 DESCRIPTION OF THE MATRIX ELEMENT

We used the maximum-likelihood program OPTIME to fit the entire $\Lambda K\pi$ Dalitz plot.[197] The model included phase space and the production of two resonances - the K^* of interest and the $Y^*(1385)$, which is produced fairly strongly in several of the final states. That is, the matrix element inserted into the program to multiply phase space was

$$Y = 1 + c_1[BW(m(K^*),\Gamma(K^*))] + c_2[BW(m(Y^*),\Gamma(Y^*))].$$

We did not allow for the distortion of phase space that is often caused by peripheral effects at high energies. We also did not allow for interference between the two resonance-production processes. Where the resonance bands cross on the Dalitz plots, no gross interference effects are evident. (Dalitz plots for the data with the "P-FID" cut make up Figure 4.8.)

4.33 SHAPE OF THE PEAK IN $m(K\pi)$

First we calculate the effect of a constant interfering background on the peak position and shape of a simple Breit-Wigner. Take an amplitude for the resonating partial wave of the form $T = x/(\epsilon - i) + (a+ib)$, where $\epsilon = (m-m_{res})/(\Gamma_{res}/2)$ and x, a, and b are real constants. The corresponding intensity is

$$I \equiv T^*T = x(x+2b)\frac{1}{\epsilon^2+1} + 2xa\frac{\epsilon}{\epsilon^2+1} + (a^2+b^2)$$

The second term reflects the distortion of the simple Breit-Wigner shape. Setting $\partial I/\partial\epsilon = 0$, we find that the peak occurs at

$$\epsilon_0 = -\frac{x+2b}{2a}\left(1 - \sqrt{(1 + [2a/(x+2b)]^2)}\right)$$

Or, for a small shift ($a << x+2b$),

$$\epsilon_0 = [a/(x+2b)] - [a/(x+2b)]^3 + \ldots$$

To see that even a small background can give a significant peak shift, consider a signal with a purely coherent and purely real background. Then at $\epsilon = 0$, $I = x^2+a^2$, and we can get ϵ_0 from the signal to background ratio:

$$\epsilon_0 = r - r^3 + \ldots, \text{ where } r = \frac{a}{x+2b} = \frac{a}{x} = \sqrt{n_B/n_S}$$

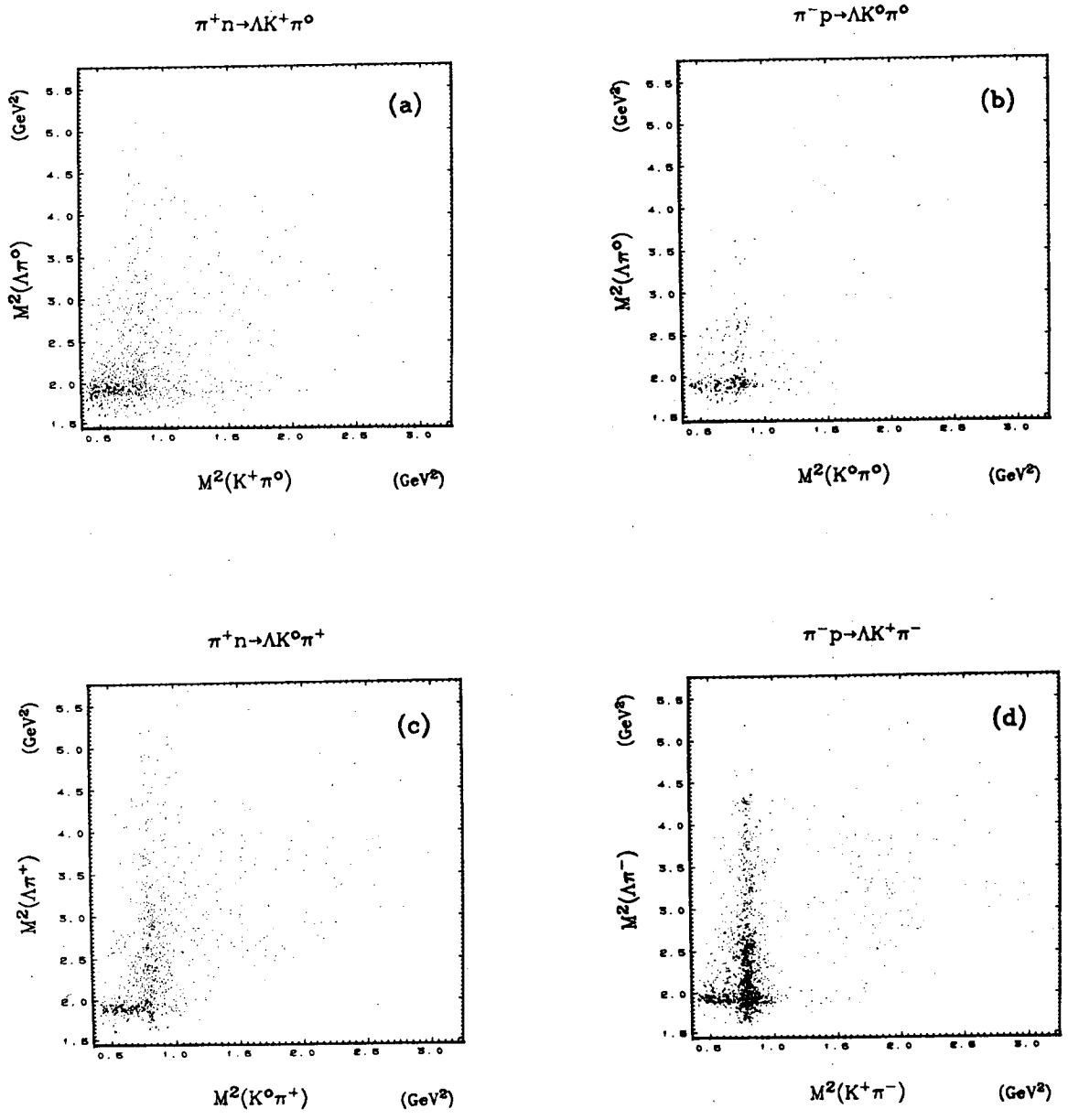

XBL 729-1811

Fig. 4.8

For example, with $\Gamma = \Gamma(K^*) = 50$ MeV,

$n_B : n_S$	ϵ_o	Peak Shift (MeV) $\delta m_o = \epsilon_o(\Gamma/2)$
1 : 1	0.618	15.5
0.1 : 1	0.290	7.2
0.01 : 1	0.099	2.5
0.001 : 1	0.032	0.8

If a rapidly varying background is involved, coherently or incoherently, the distortion of the peak can be much greater. In particular, our analysis would be invalid if there were a narrow S-wave resonance (the κ) under the K^*. A recent analysis of $K\pi$ scattering, however, does not favor the hypothesis that the κ exists.[198]

Since we are attempting to measure rather small differences in the central values of resonance shapes which have been distorted by interference, special note should be taken of the resonance shape used in the fit. We have used only the simple s-wave Breit-Wigner form, $I = 1/(\epsilon^2+1)$, where the width Γ [$\epsilon=2(m-m_{res})/\Gamma$] is constant.

This choice was originally made largely as a matter of routine and convenience, given the standard fitting program. For a measurement of the mass and not the width, the following justifications can be offered:

First, we claim that a simple Breit-Wigner that has been skewed and shifted by interference, as just described, can be adequately approximated by a simple Breit-Wigner with only a shifted central value. To demonstrate this, we have plotted both curves for various values of a peak shift. (Figure 4.9) For a specified mass shift, we calculated the amount of purely real background required to produce that shift when combined with a Breit-Wigner (solid curve). A Breit-Wigner with a shifted mass is also plotted (symmetric curve with "0"). It can be seen that for a shift of 1 MeV or less, there is no appreciable difference between the two curves. A shift of 5 MeV seems to be as large as one can handle with this simple procedure; that is approximately the size of the mass shifts which have emerged from our fits.

Clearly it would be better to take the interference into account explicitly, i.e., by introducing a simple background amplitude into the fits. However, we have no *a priori* reason to believe that the background amplitude should be particularly simple, and even a constant (complex) background requires the

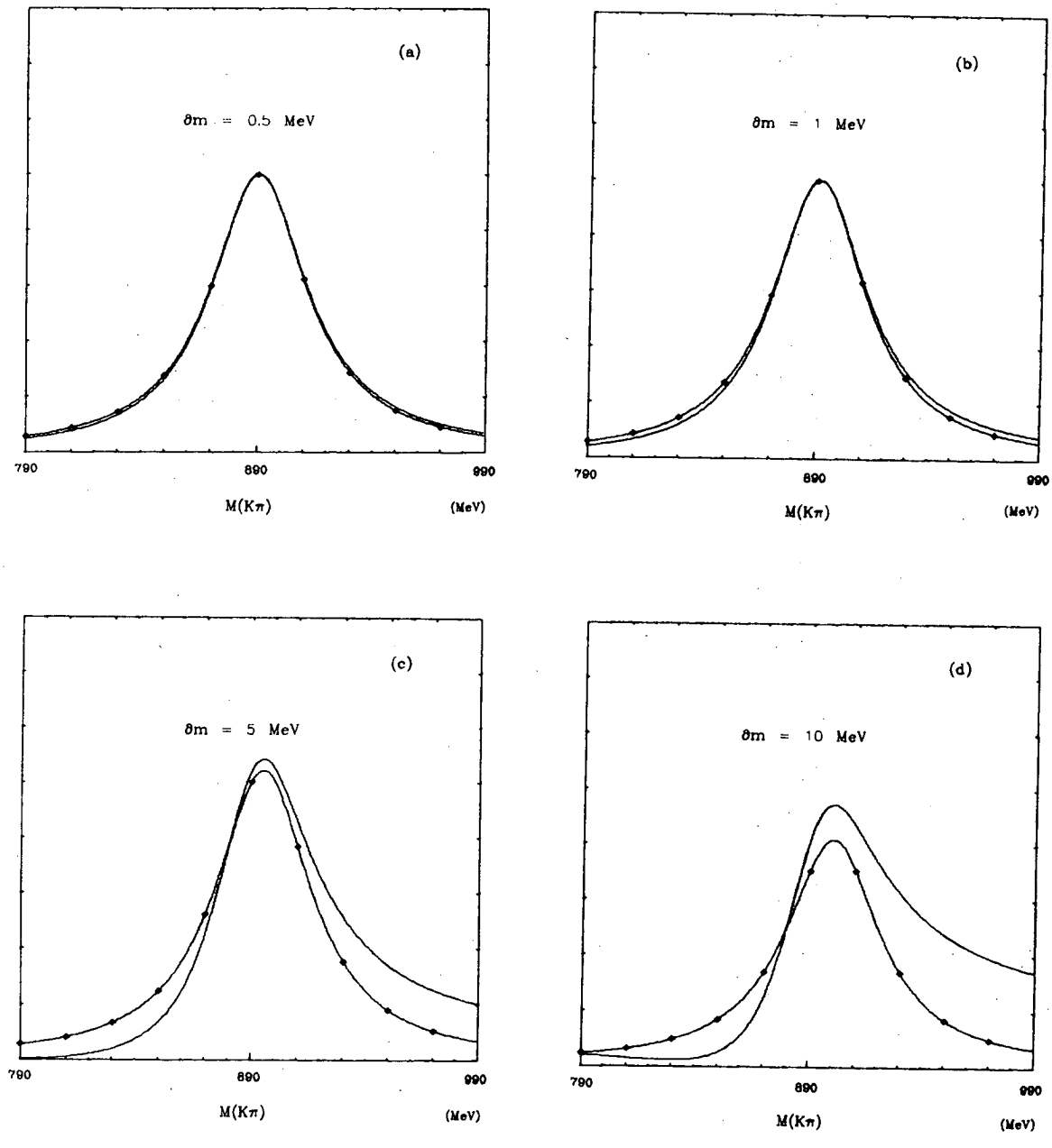

XBL 729-1682

Fig. 4.9

introduction of two additional parameters. Perhaps a proper analysis of these final states would require a study of the exact nature of the interference, but with our data we did not feel that it was called for.

A more sophisticated resonance shape would affect primarily the tails of the mass distribution. Apparently there is no single function which is unambiguously correct both below and above the peak, but the standard non-simple Breit-Wigner includes an energy-dependent width. For P-wave resonances such as the $K^*(890)$ and the $Y^*(1385)$, the width is taken to be proportional to $q^3/(1+q^2R^2)$. Here q is the c.m. momentum of the resonating particles, and R is the interaction radius, typically taken to be 1 fermi (1/(197 MeV)). Figure 4.10 shows K^* Breit-Wigners with and without this dependence. Within 50 MeV of the peak, the two curves differ only slightly, and there is no perceptible shift of the peak. We see no indication that strengthening the high-mass tails by introducing a mass-dependent width would improve the quality of our fits.[199]

The parameters varied in all the fits reported here included the relative amounts of K^* and Y^* production, and the K^* and Y^* masses. Generally, the resonance widths were held fixed at the "wallet card" values (50 MeV for the K^*, 40 MeV for the Y^*), which appear reasonably close to the observed widths. Because of the convergence problems which typically occur when maximum-likelihood programs deal with variable widths, we did only a few such fits; as we had expected, the error matrix showed little correlation between the widths and the masses. It may be hoped that the fitted K^* mass would not be shifted significantly by a symmetric error in the shape of the peak, as would result from using the wrong width or ignoring a (presumably symmetric) resolution function. As a check, we repeated 4 fits [all energies, no 1-C cut] with the K^* width held successively at 35 and 65 MeV; the fitted K^* mass was shifted by 1 MeV or less in all cases.

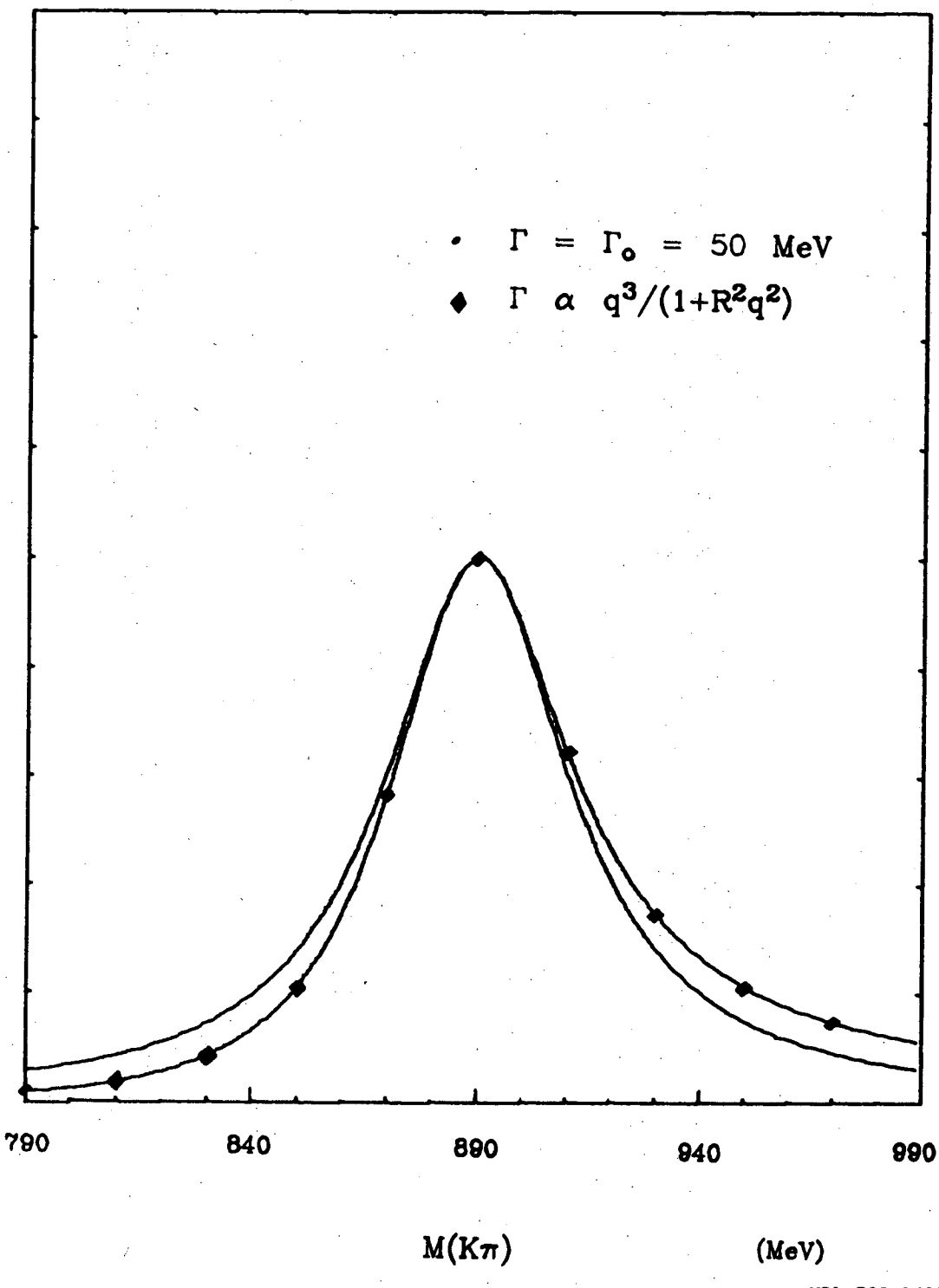

Fig. 4.10

4.34 FITTING OVER A LARGE C.M. ENERGY RANGE

As noted above, limited statistics precluded division of the data into more than two c.m. energy intervals. Each of the two regions covered a substantial range, and the variation of phase space had to be taken into account by the fitting program.

The most straightforward way of doing such a fit is to introduce an energy dependence into the matrix element and use the known distribution of path length of the incoming beam. In this case we have no interest in the energy dependence of the processes involved, and (especially for the π^+d exposure) we do not know the effective incident beam momentum distribution well. Thus, we decided to use a "normalized matrix element" to avoid complications of energy dependence.

In doing a fit at a single c.m. energy in the usual mode, OPTIME evaluates the matrix element Y for each event; the fitting process then requires that the sum of these matrix elements be divided by the integral of Y over phase space. (That integration is usually done using Monte-Carlo generated fake events.) Alternatively, one can work with a normalized matrix element, $Y_N = Y/\int Y d\rho_E$. The subscript on ρ_E is a reminder that the integration is to be done over the phase space corresponding to the c.m. energy of the event in question. We evaluated Y_N by using integrals that were stored with each event on the data tape before the fits were begun. That is, we had to integrate a constant, a K^* Breit-Wigner, and a Y^* Breit-Wigner over the phase space ρ_E for each event. Since the masses were variable, we had to evaluate the dependence of the integrals on the resonance mass. We did the integrals for the central values of the masses (m_{res}) and also for $m_{res} \pm 10$ MeV, and then applied quadratic interpolation or extrapolation at each step in the fit. (The accuracy of the interpolation procedure was confirmed by repeating the integral during the fit in several cases.) (Variable widths, when used, were handled similarly.)

4.35 ERROR ESTIMATES

The PDG has noted that several reports of masses and widths for resonances have errors that are unreasonably small, given the number of events. They pointed out that for a background-free sample of N events from a simple Breit-Wigner distribution, the minimum possible error on a determination of the central value m_o is[200]

$$\pm\delta_{min}(m_o) = \pm\sqrt{2/N}\,(\Gamma/2)$$

This follows from the fact that the minimum error in the estimator m_o^* of a

parameter m_o in any distribution $P(m,m_o)$ is given by[201]

$$\delta^2_{min}(m_o^*) = [-N \int dm\ P(m,m_o)\ \frac{\partial^2\ \ell n\ P(m,m_o)}{\partial m_o^2}]^{-1}$$

The PDG suggested that in the presence of substantial background, the minimum reasonable error is larger by about a factor of $\sqrt{2}$.

For each of the 18 fits reported here, we have calculated N, the number of K^* events, and $\delta_{min}(m_o)$. In all cases the ratio of the error from the fit to this theoretical minimum is between 1.1 and 1.7. (See Table 4.5.) Given the presence of significant background, this is on the average quite close to the "minimum reasonable error."

We note again that the error put out by the fitting program simply reflects the sensitivity of the total likelihood function (i.e., the overall fit) to a change in the K^* mass. We are, of course, particularly interested in the fit in the K^* region. In Fig. 4.11 - 4.13, we have plotted $m(K\pi)$ in 5 MeV bins. The dots are from Monte-Carlo calculations using the fitted parameters. (Unfortunately, the number of Monte-Carlo events used was not large enough to allow us to draw unambiguous smooth curves on these plots. Recall that these Monte-Carlo events were not used in the fits themselves, however.) The χ^2 for the 32 bins of each plot is indicated; the average χ^2 for the 18 fits is 43 (which, for 32 degrees of freedom, corresponds to a confidence level of about 10%).

The error from the fitting program reflects the assumption that the model is correct - that is, that the events come from a true K^*. The fact that any given sample of events fluctuates in shape from a K^* is taken into account in an average sense. The peculiarities of the specific fluctuation of the sample of course cannot be taken into account. This can be seen in Fig. 4.12(b), which is the fit we discarded because it gave an unreasonably low value for the K^* mass. From this Figure and Fig. 4.6(a) (the same data in 10 MeV bins), we see what may reasonably be interpreted as a K^* signal with an upward fluctuation in the lower half of the peak, and a downward fluctuation in the upper half. The fit gave a K^* mass of 874.7 ± 6.7 MeV, and a low χ^2 (26) in the K^* region of $m(K\pi)$. The fit gave 47 K^* events, which corresponds to δ_{min} = 5.2 MeV. Clearly nobody would expect to measure the K^* mass to 5.2 MeV from such a sample of events. However, if one had a sample of 47 events which looked like a Breit-Wigner with no apparent fluctuations, an error of 5.2 MeV would not seem unreasonable. (In that sense, it is the *minimum* error.)

As a more direct indicator of what the error from the fit means, we plotted

Reaction	1-C Cut?	$\delta_{min}m(K^*)$ (MeV) Low E <2.4 GeV	High E >2.4 GeV	All E	$\delta m(K^*)/\delta_{min}m(K^*)$ Low E <2.4 GeV	High E >2.4 GeV	All E
$\pi^+n \rightarrow \Lambda K^+\pi^o$	No	2.96 ± 0.24	3.23 ± 0.22	2.38 ± 0.14	1.65	1.36	1.38
"	Yes	4.91 ± 0.59	5.17 ± 0.53	3.70 ± 0.30	1.62	1.29	1.32
$\pi^-p \rightarrow \Lambda K^o\pi^o$	-	3.11 ± 0.24	4.00 ± 0.31	2.53 ± 0.14	1.45	1.25	1.29
$\pi^+n \rightarrow \Lambda K^o\pi^+$	No	2.07 ± 0.09	1.94 ± 0.06	1.46 ± 0.04	1.27	1.10	1.13
"	Yes	2.48 ± 0.11	2.43 ± 0.09	1.78 ± 0.05	1.22	1.10	1.15
$\pi^-p \rightarrow \Lambda K^+\pi^-$	-	1.46 ± 0.04	1.42 ± 0.03	1.05 ± 0.02	1.17	1.09	1.10

K^* Mass Errors - Theoretical Minimum and Comparison to Our Results

Table 4.5

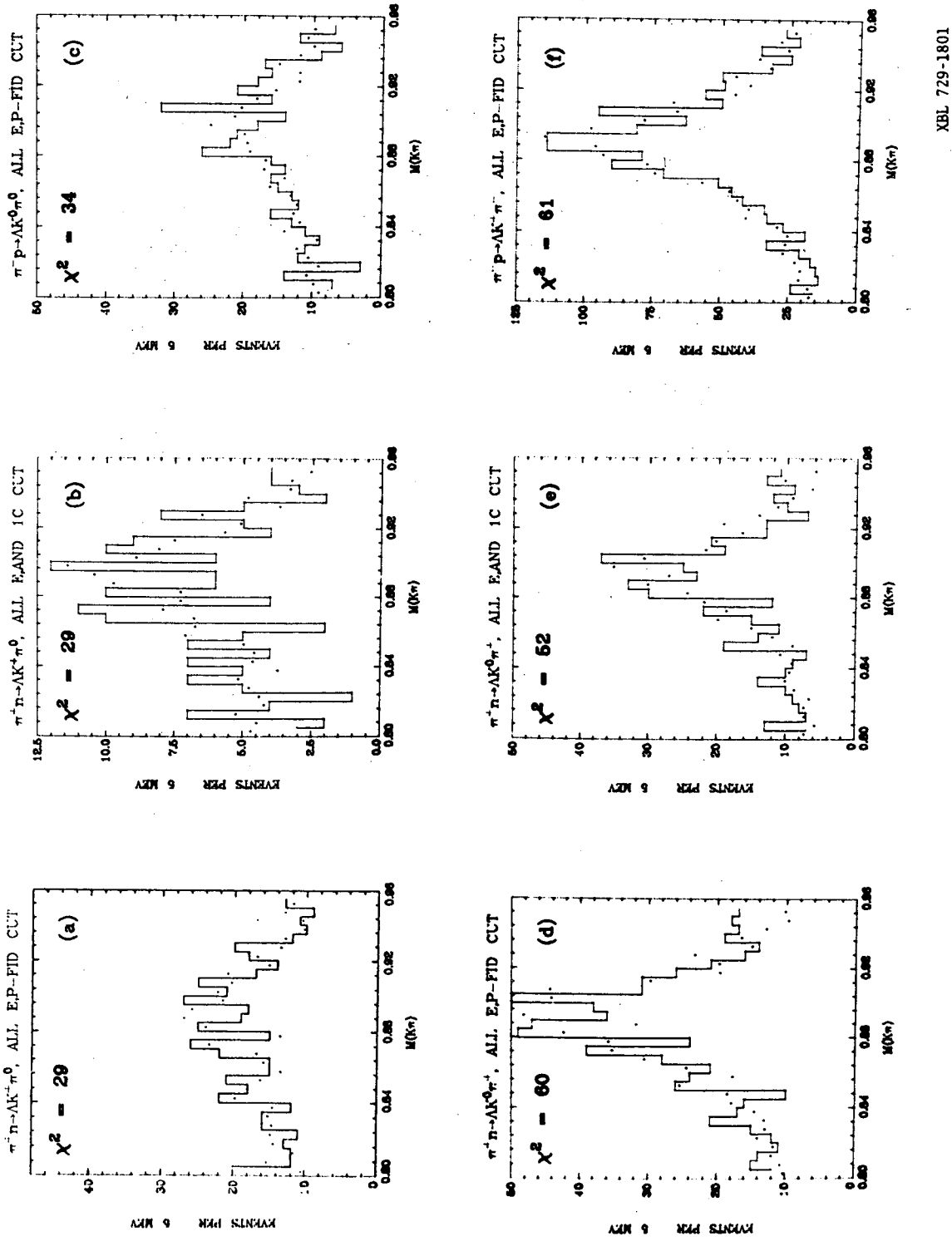

XBL 729-1801

Fig. 4.11

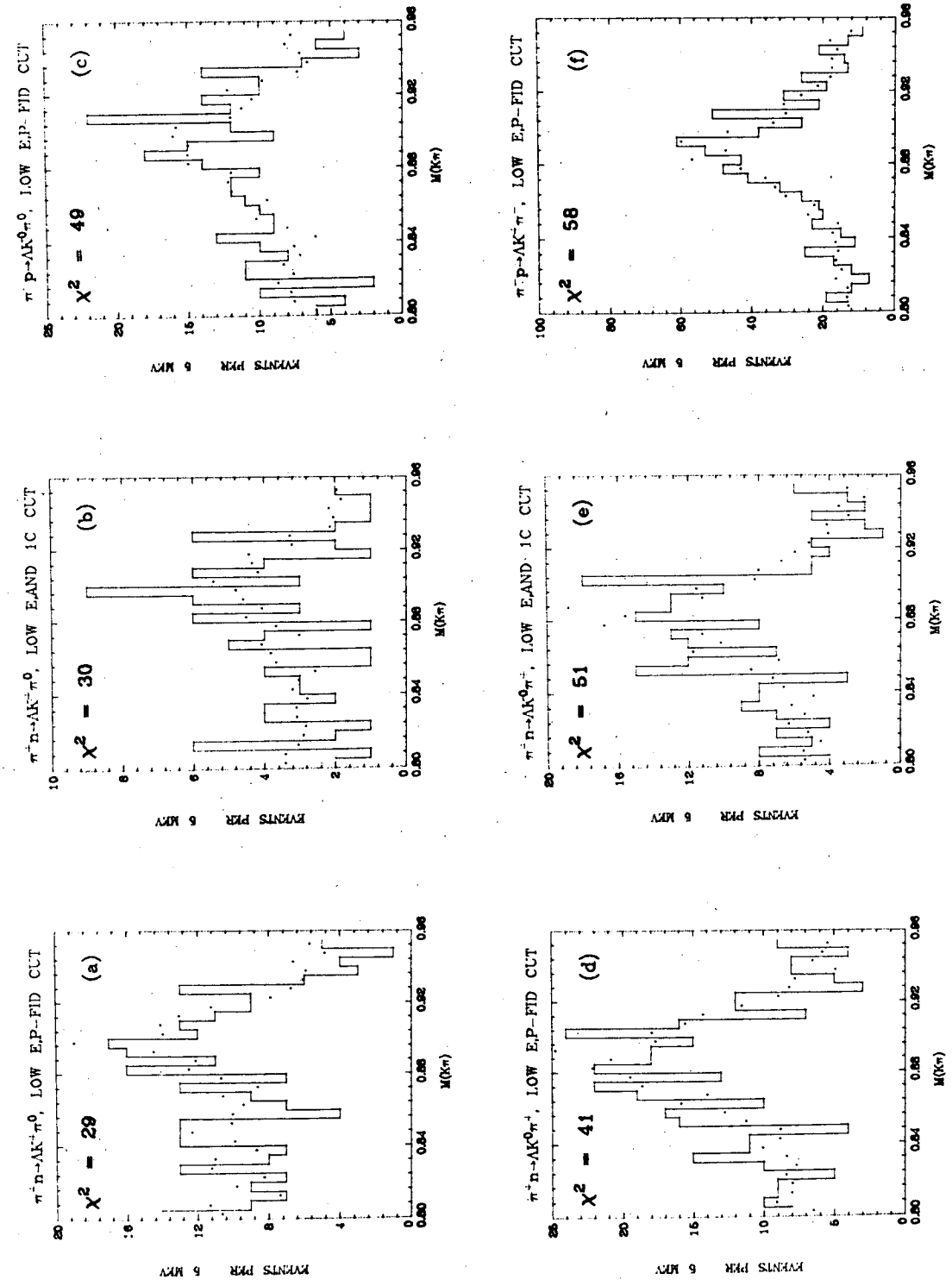

XBL 729-1802

Fig. 4.12

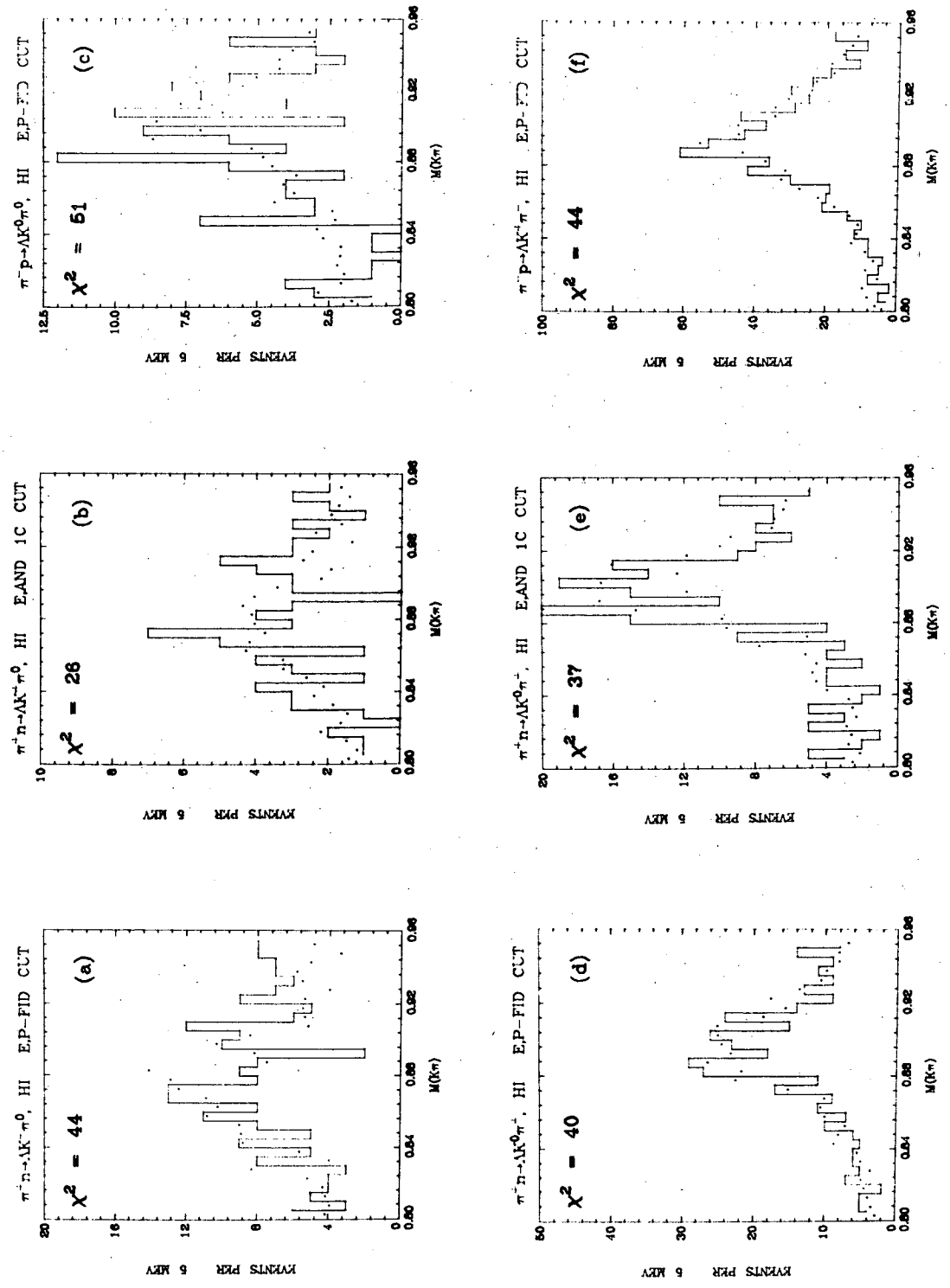
(a)
(b)
(c)
(d)
(e)
(f)
χ² = 44
χ² = 26
χ² = 51
χ² = 40
χ² = 37
χ² = 44
EVENTS PER 5 MEV
M(Kπ)
XBL 729-1803

Fig. 4.13

some of the data with curves corresponding to the results of the fit and also curves corresponding to a shift of 1, 2, or 3 standard deviations in the K^* mass. Because the events are not distributed smoothly and symmetrically, such shifts do not make the fit look much worse.

From these observations, we concluded that it would be reasonable to double all the errors on $m(K^*)$. As noted in Section 4.2, we subsequently saw that this "scale factor" of 2 brings our three independent results for the mass difference into agreement, within errors.

4.36 ADDITIONAL ANALYSIS CONSIDERED

In this section we mention some further work which we considered but did not complete. We studied the possibility of using a different fitting method, and of getting additional information from 4-body final states.

The reactions reported above have allowed us to study both decay modes of the K^{*+} in a π^+n reaction, and both modes of the K^{*o} in π^-p. As a hedge against systematic effects, it would have been nice to measure the mass of the K^{*o} in a π^+n reaction, and K^{*+} in π^-p. The only pair of three-body final states for which this is possible is $\pi^+n \rightarrow \Sigma^+K^o\pi^o$ and $\pi^-p \rightarrow \Sigma^-K^+\pi^o$. (The reaction $\pi^+d \rightarrow (p)\Sigma^+K^+\pi^-$ has not been measured in our experiment.) However, we assigned only 65 events to the former reaction. Turning to the four-body final states, we find two candidate pairs of reactions:

$$\pi^+ \; n \longrightarrow \Lambda \; \pi^+ \; (K^o \; \pi^o) \qquad (\; 303)$$
$$\pi^- \; p \longrightarrow \Lambda \; \pi^- \; (K^+ \; \pi^o) \qquad (1438)$$

$$\pi^+ \; n \longrightarrow \Lambda \; \pi^+ \; (K^+ \; \pi^-) \qquad (1019)$$
$$\pi^- \; p \longrightarrow \Lambda \; \pi^- \; (K^o \; \pi^+) \qquad (2258)$$

The number of events in the raw data is indicated for each reaction. The number of events is clearly inadequate in the first case. Analysis of the second pair of reactions is complicated by the large number of final-state resonances that can be, and in fact are, produced. There are definite but hardly impressive K^* signals. (The $K\pi$ mass spectra are shown in Figure 4.14.) We have done no work on these reactions.

In four-body reactions, it is not easy to do a fit to the entire final state. Therefore, we considered fitting just part of the $m(K\pi)$ spectrum. We attempted to test this method on the three-body states. We used the same function as

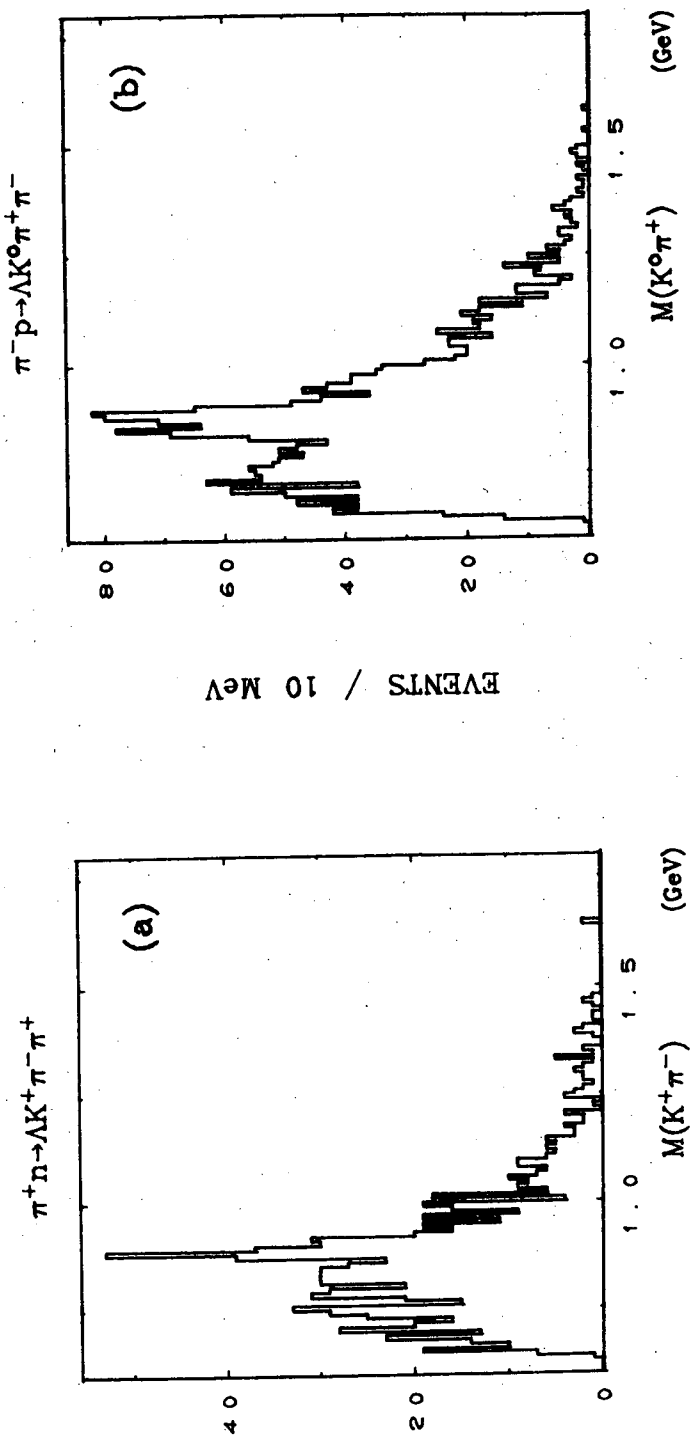
(b)
$\pi^- p \to \Lambda K^0 \pi^+ \pi^-$
EVENTS / 10 MeV
$M(K^0\pi^+)$ (GeV)
(a)
$\pi^+ n \to \Lambda K^+ \pi^- \pi^+$
EVENTS / 10 MeV
$M(K^+\pi^-)$ (GeV)
XBL 729-1812

Fig. 4.14

Barash *et al.*,[202]

$$f(m) = (a+b\epsilon)/(\epsilon^2+1) + (c_1 + c_2 m + c_3 m^2), \qquad (4.5)$$

where $\epsilon = (m-m_{res})/(\Gamma/2)$, as usual, and $m \equiv m(K\pi)$. The term with the coefficient b explicitly takes into account a constant interfering background. Our limited work with fits using this function was not successful; apparently our fitting program could not easily distinguish a Breit-Wigner from a quadratic background.

4.4 EVALUATION AND COMPARISON WITH OTHER RESULTS

One can make the following general criticism of the result we have presented:

(1) By using a fixed-width S-wave Breit-Wigner, we may have come perilously close to ignoring the effect we are most concerned with. This is true even though the distortion due to interference should cancel out, and an unmodified but shifted Breit-Wigner is a reasonable approximation to a distorted curve with a peak shift of a few MeV. In other words, no real check has been made on the validity of our model. One reason for our simplified treatment was the lack of enough events to study the resonance shape carefully. Another was the technical problems involved in fitting various complicated shapes over a wide c.m. energy band. (We had to integrate the Breit-Wigner over phase space for several values of all of its variable parameters.)

(2) Our charge-symmetric pairs of reactions do not have essentially identical mass spectra, even for the $K\pi$ mass outside the K^*. (Recall that the pseudo-1C cut did decrease the discrepancy.) That is, the charge symmetry which is the key to this determination is not well reflected by the data.

(3) The quality of the fits is no better than adequate.

(4) We did not examine systematic effects other than interference. The only evidence that such effects are not serious is the fact that the Y^* mass difference determinations look good. A proper determination of a resonance mass to within a few MeV with bubble chamber data should take into account many possible biases, such as distortions due to treatment of a spectator nucleon, topology-dependent effects, and experiment-dependent effects such as errors in the magnetic field.[203]

As noted in the introduction, when we decided to do this study there were only three reported determinations of the K^* mass difference. Two of them were by Ficenec *et al.*, who studied the reactions $K^-p \rightarrow K^{*-}p$ and $K^{*0}n$ at 1.3 and 2.7 GeV/c.[204,205] Their primary interest in fitting these final states appears to

have been determination of the production cross section for various resonances. First the Dalitz plot was fit to phase space plus five resonances, with only the amounts varying; then the $K\pi$ mass spectrum was fit, with the K^* mass and width being varied. Apparently no special steps were taken because of possible interference. The resonance form used was a modified Breit-Wigner.

For their low-momentum data, Ficenec noted that "little significance can be attached to the mass difference $\bar{K}^{*0} - \bar{K}^{*-} = 6 \pm 4$ MeV since the width of the $\bar{K}^*$ and the experimental resolution are large." In fact, the quoted mass errors are not inconsistent with the reasonable minimum that can be deduced from the number of events and the width. (At the higher momentum, no such explicit disclaimer was made in connection with the quoted result of (10 ± 4) MeV, although the same reasoning presumably is still valid; here the PDG did scale up one of the mass errors. Further increasing the errors because the K^{*0} masses at 1.3 and 2.7 GeV/c did not agree, the PDG used (6.5 ± 5) MeV and (9.5 ± 5) MeV in the compilation.) Although K^* production was the dominant process at both momenta, there was enough background so that interference effects can not safely be ignored. We agree with the PDG's conclusion that this result should not be given too much weight, but not for the reason cited in the original paper.

The remaining published value of Δm is that of Barash *et al.*, who reported $\Delta m = (6.3 \pm 4.1)$ MeV.[202] (The error was increased to 6 MeV in the PDG compilation.) They observed both the charged and neutral K^* in each of two final states:

$$\bar{p}\, p \longrightarrow \bar{K}^0\, K^+\, \pi^- \quad \text{and} \quad \bar{p}\, p \longrightarrow K^0\, K^-\, \pi^+ \qquad (4.6)$$

Although the two final states are charge-symmetric to each other, the charge symmetry of the strong interactions does not require any peak shifting due to background to be the same in the two cases. That principle applies to the reactions $\bar{p}p \rightarrow \bar{K}^0K^+\pi^-$ and $\bar{n}n \rightarrow K^0K^-\pi^+$, and also to the reactions $\bar{p}p \rightarrow K^0K^-\pi^+$ and $\bar{n}n \rightarrow \bar{K}^0K^+\pi^-$.[206]

Barash *et al.* fit a 420-MeV interval of the $K\pi$ mass spectrum to a Breit-Wigner plus a skewing term, plus a quadratic background. (See equation 4.5.) Note that this skewing term did allow for a peak shift due to interference. However, it is not clear from Ref. 202 how well this method worked.[207] To evaluate the result, one would like to know how much of the interference term was required, what the apparent K^* mass was, and how good the fits were. Favorable features of their result include a good K^* signal with a background rather independent of $m(K\pi)$, and the fact that both charge states were observed

not only in the same experiment but in the same final state. Barash *et al.* noted, as a check against systematic effects, that the mass differences for the particle-antiparticle K^* pairs were consistent with zero.

After the completion of our analysis, we learned of what appears to be a definitive study of the K^* mass difference. Aguilar-Benitez, Eisner, and Kinson (AEK) have studied the properties of the $K^*(890)$ and the $K^*(1420)$ in a K^-p bubble chamber exposure at 3.9 and 4.6 GeV/c.[208] From the $NK\pi$ final states, they obtain a mass difference of

$$\Delta m = m(K^{*o}) - m(K^{*-}) = (5.7 \pm 1.7) \text{ MeV}.$$

In its treatment of all problems involved in this determination except that of a peak shift due to intererence, this report is clearly a great deal better than previous studies, including ours. Aguilar-Benitez had high statistics ($\approx$2900 K^{*o} events and $\approx$4400 K^{*-} events), with little background ($\approx$11% and $\approx$7% respectively). They investigated the effects of using a simple Breit-Wigner rather than an energy-dependent one; the simple form gave a consistent mass difference, $\Delta m = (6.8 \pm 1.0)$ MeV. They measured the K^{*o} mass in topologies with and without a visible K^o decay, and the K^{*o} mass in a four-body final state also, finding excellent agreement.

AEK did not make any explicit reference to a possible peak shift due to background. However, the small background level puts limits on this peak shift. The worst possible case would occur if all the background at the K^* comes from a purely real I=3/2 P wave; the maximum peak shift would be 9 MeV. (This estimate is from the formulas of Section 4.33, which apply to a mass-independent background.) If no more than 5% of the background events are interfering, the peak shift would have to be less than 2 MeV, the quoted error in Δm. AEK have since reported that they have been able to understand the K^* decay distributions by taking all the background to be S-wave.[209] (There is a noticeable asymmetry in the decay cosine.) That is, there is little or none of the amplitude which may produce a peak shift.

When we began this work, we were aware that a better study would probably be done in the future. H. Taft and others had suggested looking at $K^{\pm}d \rightarrow K^{*\pm}d$ and $K^o_L d \rightarrow K^{*o}d$.[210] Not only are the reactions charge-symmetric, but only I=1/2 amplitudes are present, so there should be no problems at all with interference. (One of the many reasons we did not push our limited data very hard was that this experiment was anticipated.)

The average of the 3 early determinations of Δm, as compiled by the PDG,

was (7.6 ± 3.0) MeV; including the AEK result, it is (6.1 ± 1.5) MeV. (We have not included a very recent result reported by Engelmann *et al.*[211]) Our result, (-2.7 ± 4.4) MeV, is in disagreement with the world average by about 2 standard deviations. Including our result, the average is (5.2 ± 1.4) MeV. Before we learned of the AEK result, we had concluded that although our measurement was not particularly good, it did cast some doubt on the 3 previous results. We now feel the systematic uncertainties discussed above have probably resulted in the wrong answer in our determination.

ACKNOWLEDGEMENTS

I am grateful to Art Rosenfeld, who suggested this study; Odette Benary, who worked on the early stages of the analysis; and Werner Koellner, who helped me with the fitting program.

I would like to incorporate by reference the acknowledgements in Chapter 2, thanking the many people who helped at various times during the analysis and the preparation of this report.

This work was performed under the auspices of the U.S. Atomic Energy Commission.

REFERENCES

1-180. These numbers were reserved for Chapters 1 through 3 of this thesis (LBL-1051 and 1052).

181. Particle Data Group, Review of Particle Properties, Rev. Mod. Phys. 42, 87 (1970), p. 151.

182. Stan Flatté, LBL Group A Memo 711 (1970).

183. P. J. Biggs *et al.*, Phys. Rev. Letters 24, 1201 (1970).

184. Particle Data Group, Review of Particle Properties, Phys. Letters 39B, 1 (1972), p. 56.

185. These are some of the predictions cited in Refs. 182 and 202 and are not intended to be a summary of the theoretical situation. Additional discussion can be found in Ref. 211.

186. See Ref. 182, p. 3, and S. Coleman *et al.*, 'Proceedings of the International Conference on High-Energy Physics,' Dubna (1964), Vol. I, p. 785.

187. F. Duimio and A. Scotti, Phys. Rev. Letters 14, 926 (1965).

188. Sudesh Bose, Phys. Rev. 140, B349 (1965).

189. H. Harari, Phys. Rev. 139, B1323 (1965).

190. H. R. Rubinstein, Phys. Rev. Letters 17, 41 (1966).

191. Particle Data Group, Review of Particle Properties, Phys. Letters 33B, 1 (1970), p. 73.

192. Chapter 2 of this thesis is in LBL Report LBL-1051; see Section 2.82 for the values of the separation parameters used. (We used the May 1970 edition of our data tape; a minor bug was corrected before the final data tape was made.)

193. Donald W. Davies (Ph. D. thesis), LBL Report UCRL-19263 (1969). Published version: Davies *et al.*, Phys. Rev. D2, 506 (1970).

194. Lyndon M. Hardy (Ph. D. thesis), LBL Report UCRL-16788 (1966); the results are published in Dahl *et al.*, Phys. Rev. 163, 1377 (1967).

195. Chapter 2 of this thesis (Ref. 192), Sections 7 and 10.

196. Ref. 184 (PDG Compilation), p. 11.

197. Philippe H. Eberhard and Werner O. Koellner, LBL Reports UCRL-20159 and 20160 (1970).

198. Maxine Matison, LBL, private communication.

199. See Fig. 4.1. The effects of such factors on the apparent K^* mass are discussed by Aguilar-Benitez *et al.* (Ref. 208) and by Engelmann *et al.*

(Ref. 211).

200. Ref. 181, p. 151.

201. The derivation of the result for a Breit-Wigner from this principle was provided to me by Gerry Lynch.

202. N. Barash *et al.*, Phys. Rev. 156, 1399 (1967), p. 1404.

203. As an example of the kind of systematic effect that may be important, we note that in our low-momentum $\pi^+ d$ exposure there was a small shift in the ω mass when the wrong beam momentum was used in beam averaging (i.e., as a second measurement of the beam-track momentum). (Jerry Danburg, private communication.)

204. J. R. Ficenec *et al.*, Phys. Rev. 169, 1034 (1968).

205. J. R. Ficenec *et al.*, Phys. Rev. 175, 1725 (1968).

206. The January 1970 edition of the PDG compilation (Ref. 181) incorrectly implied that the Barash result was not subject to the uncertainty due to interference that limited the Ficenec results. See Ref. 210 for clarification of this point.

207. N. Barash (Ph. D. thesis), Columbia Univ. Report CU-1932-261 (1967).

208. M. Aguilar-Benitez, R. L. Eisner, and J. B. Kinson, Phys Rev. D4, 2583 (1971).

209. M. Aguilar-Benitez, S. U. Chung, and R. L. Eisner, Phys. Rev. D6, 11 (1972).

210. A. H. Rosenfeld and P. Söding, Measurement of the (K^{*o}-$K^{*\pm}$) Mass Splitting: Two proposed experiments which are safe from interference, LBL Group A Memo 705 (1970).

211. R. Engelmann *et al.*, Phys. Rev. D5, 2162 (1972). Interference effects were not included in their fits; they noted theoretical calculations predicting that they should be small ($\lesssim$2 MeV). They reported Δm = (7.5 ± 2.0) MeV and (10.3 ± 3.3) MeV.

FIGURE AND TABLE CAPTIONS

Fig. 4.1 (Page 9)

The m(Kπ) spectrum for each of the 4 K^* production reactions, for all c.m. energies combined. The dots are fake events generated using the parameters determined by the fits.

Fig. 4.2 through 4.4 (Pp. 10-12)

Same as Fig. 4.1, but showing the other mass spectra [m($\Lambda\pi$), m(ΛK)] and the c.m. energy respectively.

Fig. 4.5 (Page 13)

M(Kπ), as in Fig. 4.1, but without the "pseudo-one-constraint" cut in (a,c); (b,d) are the same as in Fig. 4.1.

Fig. 4.6 (Page 14)

M(Kπ), as in Figs. 4.1 and 4.5, but for the low-energy sample only.

Fig. 4.7 (Page 15)

M(Kπ), as in Figs. 4.1 and 4.5, but for the high-energy sample only.

Fig. 4.8 (Page 20)

Dalitz plots for the 4 K^* production reactions.

Fig. 4.9 (Page 22)

Comparison of a Breit-Wigner resonance shape skewed by interference (plain curves) with a shifted but undistorted Breit-Wigner (curves with "0"). The amount of the shift is (a): 0.5 MeV; (b): 1 MeV; (c): 5 MeV; (d): 10 MeV.

Fig. 4.10 (Page 24)

Comparison of Breit-Wigners for the $K^*(890)$ with fixed width (plain curve) and variable width (curve with "0").

TECHNICAL INFORMATION DIVISION
LAWRENCE BERKELEY LABORATORY
UNIVERSITY OF CALIFORNIA
BERKELEY, CALIFORNIA 94720